The Phosphatase PP1 Promotes Mitotic Slippage through Mad3 Dephosphorylation

Antonella Ruggiero, Yuki Katou, Katsuhiko Shirahige, Martial Séveno, Simonetta Piatti

Current Biology

The phosphatase PP1 promotes mitotic slippage through Mad3 dephosphorylation

--Manuscript Draft--

Manuscript Number:	CURRENT-BIOLOGY-D-19-00907R2
Full Title:	The phosphatase PP1 promotes mitotic slippage through Mad3 dephosphorylation
Article Type:	Report
Corresponding Author:	Simonetta Piatti, PhD CNRS Montpellier, FRANCE
First Author:	Antonella Ruggiero
Order of Authors:	Antonella Ruggiero
	Yuki Katou
	Katsuhiko Shirahige
	Martial Sevéno
	Simonetta Piatti, PhD
Abstract:	Accurate chromosome segregation requires bipolar attachment of kinetochores to spindle microtubules. A conserved surveillance mechanism, the Spindle Assembly Checkpoint (SAC), responds to lack of kinetochore-microtubule connections and delays anaphase onset until all chromosomes are bipolarly attached [1]. SAC signalling fires at kinetochores and involves a soluble Mitotic Checkpoint Complex (MCC) that inhibits the Anaphase-Promoting Complex (APC) [2,3]. The mitotic delay imposed by SAC, however, is not everlasting. If kinetochores fail to establish bipolar connections, cells can escape from the SAC-induced mitotic arrest through a process called mitotic slippage [4]. Mitotic slippage occurs in the presence of SAC signalling at kinetochores [5,6], but whether and how MCC stability and APC inhibition are actively controlled during slippage is unknown. The PP1 phosphatase has emerged as a key factor in SAC silencing once all kinetochores are bipolarly attached [7,8]. PP1 turns off SAC signalling through dephosphorylation of the SAC scaffold Knl1/Blinkin at kinetochores [9–11]. Here we show that in budding yeast PP1 is also required for mitotic slippage. However, its involvement in this process is not linked to kinetochores but rather to MCC stability. We identify S268 of Mad3 as a critical target of PP1 in this process. Mad3 S268 dephosphorylation destabilises the MCC without affecting the initial SAC-induced mitotic arrest. Conversely, it accelerates mitotic slippage and overcomes the slippage defect of PP1 mutants. Thus, slippage is not the mere consequence of incomplete APC inactivation that brings about mitotic exit, as originally proposed, but involves the exertive antagonism between kinases and phosphatases.

CELL PRESS DECLARATION OF INTERESTS POLICY

Transparency is essential for a reader's trust in the scientific process and for the credibility of published articles. At Cell Press, we feel that disclosure of competing interests is a critical aspect of transparency. Therefore, we ask that all authors disclose any financial or other interests related to the submitted work that (1) could affect or have the perception of affecting the author's objectivity, or (2) could influence or have the perception of influencing the content of the article, in a "Declaration of Interests" section.

What types of articles does this apply to?

We ask that you disclose competing interests for all submitted content, including research articles as well as front matter (e.g., Reviews, Previews, etc.) by completing and submitting the "Declaration of Interests" form below. We also ask that you include a "Declaration of Interests" section in the text of all research articles even if there are no interests declared. For front matter, we ask you to include a "Declaration of Interests" section only when you have information to declare.

What should I disclose?

We ask that you and all authors disclose any personal financial interests (examples include stocks or shares in companies with interests related to the submitted work or consulting fees from companies that could have interests related to the work), professional affiliations, advisory positions, board memberships, or patent holdings that are related to the subject matter of the contribution. As a guideline, you need to declare an interest for (1) any affiliation associated with a payment or financial benefit exceeding $10,000 p.a. or 5% ownership of a company or (2) research funding by a company with related interests. You do not need to disclose diversified mutual funds, 401ks, or investment trusts.

Where do I declare competing interests?

Competing interests should be disclosed on the "Declaration of Interests" form as well as in the last section of the manuscript before the "References" section, under the heading "Declaration of Interests". This section should include financial or other competing interests as well as affiliations that are not included in the author list. Examples of "Declaration of Interests" language include:

> "AUTHOR is an employee and shareholder of COMPANY."
> "AUTHOR is a founder of COMPANY and a member of its scientific advisory board."

NOTE: Primary affiliations should be included on the title page of the manuscript with the author list and do not need to be included in the "Declaration of Interests" section. Funding sources should be included in the "Acknowledgments" section and also do not need to be included in the "Declaration of Interests" section. (A small number of front-matter article types do not include an "Acknowledgments" section. For these articles, reporting of funding sources is not required.)

What if there are no competing interests to declare?

For *research* articles, if you have no competing interests to declare, please note that in a "Declaration of Interests" section with the following wording:

> "The authors declare no competing interests."

Front-matter articles do not need to include this section when there are no competing interests to declare.

CELL PRESS DECLARATION OF INTERESTS FORM

If submitting materials via Editorial Manager, please complete this form and upload with your final submission. Otherwise, please e-mail as an attachment to the editor handling your manuscript.

Please complete each section of the form and insert any necessary "Declaration of Interest" statement in the text box at the end of the form. A matching statement should be included in a "Declaration of Interest" section in the manuscript.

Institutional Affiliations

We ask that you list the current institutional affiliations of all authors, including academic, corporate, and industrial, on the title page of the manuscript. ***Please select one of the following:***

- (●) All affiliations are listed on the title page of the manuscript.
- ( ) I or other authors have additional affiliations that we have noted in the "Declaration of Interests" section of the manuscript and on this form below.

Funding Sources

We ask that you disclose all funding sources for the research described in this work. ***Please confirm the following:***

- (●) All funding sources for this study are listed in the "Acknowledgments" section of the manuscript.*

*A small number of front-matter article types do not include an "Acknowledgments" section. For these, reporting funding sources is not required.

Competing Financial Interests

We ask that authors disclose any financial interests, including financial holdings, professional affiliations, advisory positions, board memberships, receipt of consulting fees etc., that:

(1) could affect or have the perception of affecting the author's objectivity, *or*
(2) could influence or have the perception of influencing the content of the article.

Please select one of the following:

- (●) The authors have no financial interests to declare.
- ( ) I or other authors have noted any financial interests in the "Declaration of Interests" section of the manuscript and on this form below.

Advisory/Management and Consulting Positions

We ask that authors disclose any position, be it a member of a Board or Advisory Committee or a paid consultant, that they have been involved with that is related to this study. ***Please select one of the following:***

- (●) The authors have no positions to declare.
- ( ) I or other authors have management/advisory or consulting relationships noted in the "Declaration of Interests" section of the manuscript and on this form below.

Patents

We ask that you disclose any patents related to this work by any of the authors or their institutions. ***Please select one of the following:***

- (●) The authors have no related patents to declare.
- ( ) I or one of my authors have a patent related to this work, which is noted in the "Declaration of Interests" section of the manuscript and on this form below.

Please insert any "Declaration of Interests" statement in this space. This exact text should also be included in the "Declaration of Interests" section of the manuscript. If no authors have a competing interest, please insert the text, "The authors declare no competing interests."

The authors declare no competing interests

On behalf of all authors, I declare that I have disclosed all competing interests related to this work. If any exist, they have been included in the "Declaration of Interests" section of the manuscript.

Name: Simonetta Piatti

Manuscript Number (if available): CURRENT-BIOLOGY-D-19-00907R1

Graphical Abstract

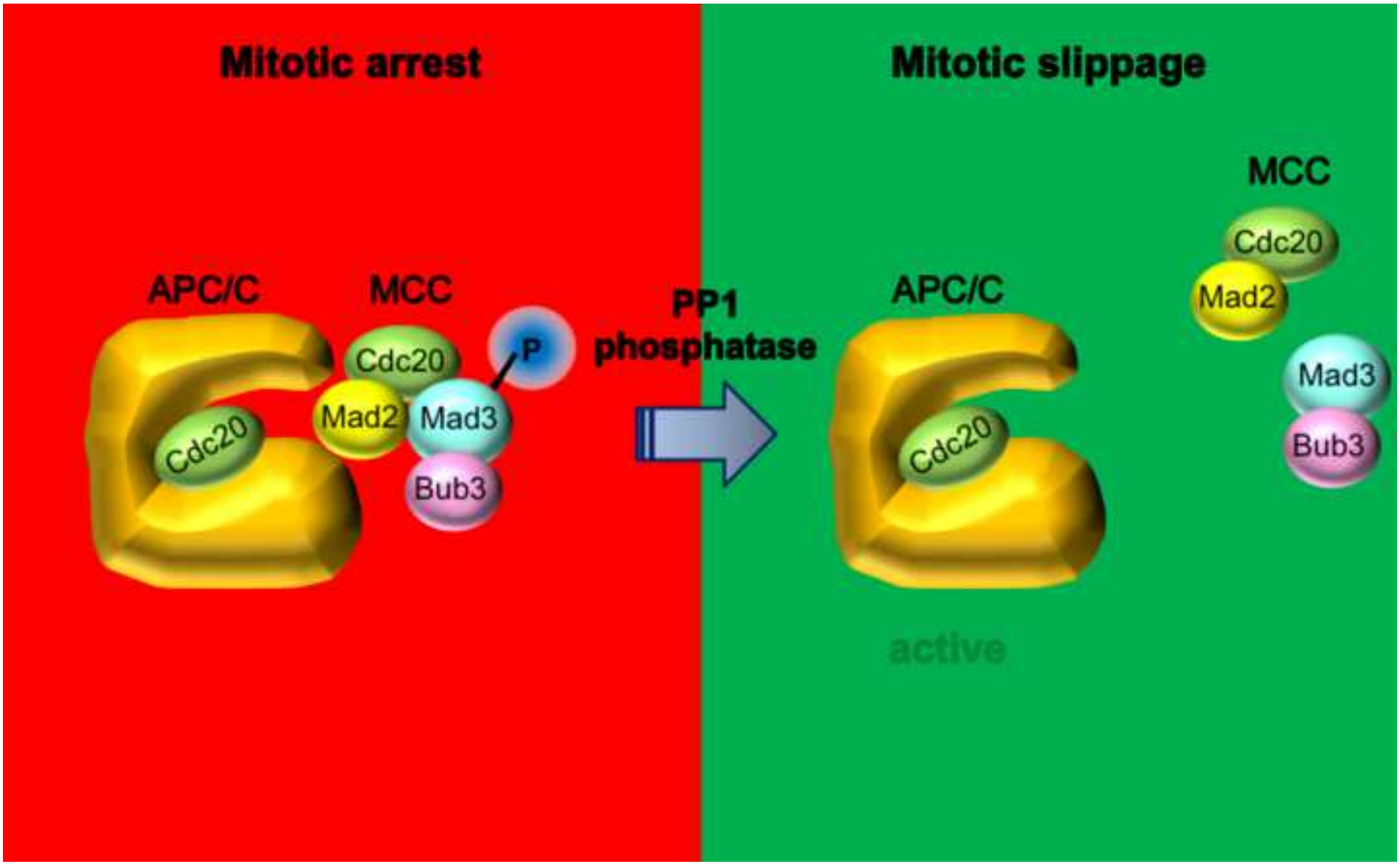

The phosphatase PP1 promotes mitotic slippage through Mad3 dephosphorylation

Antonella Ruggiero, Yuki Katou[1], Katsuhiko Shirahige[1], Martial Séveno[2] and Simonetta Piatti[3]

Centre de Recherche en Biologie Cellulaire de Montpellier (CRBM)

1919 Route de Mende

34293 Montpellier (France)

[1]Research Center for Epigenetic Disease

University of Tokyo

1-1-1 Yayoi, Bunkyo-ku

113-0032 Tokyo (Japan)

[2]BioCampus Montpellier, CNRS, INSERM, Montpellier University,

34000 Montpellier (France)

[3]Lead contact: simonetta.piatti@crbm.cnrs.fr

SUMMARY

Accurate chromosome segregation requires bipolar attachment of kinetochores to spindle microtubules. A conserved surveillance mechanism, the Spindle Assembly Checkpoint (SAC), responds to lack of kinetochore-microtubule connections and delays anaphase onset until all chromosomes are bipolarly attached [1]. SAC signalling fires at kinetochores and involves a soluble Mitotic Checkpoint Complex (MCC) that inhibits the Anaphase-Promoting Complex (APC) [2,3]. The mitotic delay imposed by SAC, however, is not everlasting. If kinetochores fail to establish bipolar connections, cells can escape from the SAC-induced mitotic arrest through a process called mitotic slippage [4]. Mitotic slippage occurs in the presence of SAC signalling at kinetochores [5,6], but whether and how MCC stability and APC inhibition are actively controlled during slippage is unknown. The PP1 phosphatase has emerged as a key factor in SAC silencing once all kinetochores are bipolarly attached [7,8]. PP1 turns off SAC signalling through dephosphorylation of the SAC scaffold Knl1/Blinkin at kinetochores [9–11]. Here we show that in budding yeast PP1 is also required for mitotic slippage. However, its involvement in this process is not linked to kinetochores but rather to MCC stability. We identify S268 of Mad3 as a critical target of PP1 in this process. Mad3 S268 dephosphorylation destabilises the MCC without affecting the initial SAC-induced mitotic arrest. Conversely, it accelerates mitotic slippage and overcomes the slippage defect of PP1 mutants. Thus, slippage is not the mere consequence of incomplete APC inactivation that brings about mitotic

exit, as originally proposed, but involves the exertive antagonism between kinases and phosphatases.

RESULTS AND DISCUSSION

The PP1 phosphatase is required for mitotic slippage in budding yeast

Mitotic slippage occurs when SAC is not satisfied for a prolonged time [12]. In mammalian cells and budding yeast it ensues in the presence of SAC proteins bound to kinetochores (e.g. Mad2), which led to the proposal that SAC keeps signalling under these conditions [5,6]. Given its crucial role in SAC silencing [7–9,11], we asked if PP1 is involved also in mitotic slippage in budding yeast. To follow mitotic slippage, we activated SAC by *MAD2* overexpression from the galactose-inducible *GAL1* promoter (i.e. in the absence of spindle damage) or microtubule-depolymerizing drugs (e.g. benomyl) [13]. Under these conditions, wild type cells arrested transiently in mitosis as large budded cells with high levels of cyclin B (Clb2) and securin (Pds1) (Figure 1A-B, D). After a few hours, however, they slipped out of mitosis through cyclin B and securin degradation, as well as accumulation of the CDK inhibitor Sic1, a marker of G1 (Figure 1A)[14]. Afterwards, cells progressively formed microcolonies (Figure 1D, [13]).

We inactivated the PP1 catalytic subunit Glc7 through the temperature-sensitive *glc7-10* that is defective in SAC silencing at 30°C [7]. PP1 inhibition delayed mitotic slippage, as shown by the slower degradation of Pds1 and Clb2 and sluggish re-accumulation of Sic1 in the presence of benomyl (Figure 1A). Furthermore, while wild type cells divided and gathered aberrant DNA contents, *glc7-10* cells remained arrested for longer times with post-replicative DNA contents (Figure 1B). Microcolony assays and live cell imaging upon *MAD2* overexpression showed that

glc7-10 cells could not slip out of mitosis and remained arrested as large budded cells throughout the duration of the experiment (Figure 1D) and eventually died (Video S1). Consistently, *MAD2* overexpression was lethal for *glc7-10* mutant but not for wild type cells (Figure 1C).

Thus, PP1 is required for timely mitotic slippage as it is for SAC silencing.

The role of PP1 in mitotic slippage is not linked to SAC signalling at kinetochores

Upon SAC activation, phosphorylation of the kinetochore scaffold Spc105/Knl1, which is counteracted by PP1, brings about the sequential recruitment of the SAC complex Bub3-Bub1 followed by Mad1 [10,15–18]. Thus, binding of Mad1 to Bub3 or Bub1 takes place only when SAC is signalling. We previously showed that the Mad1-Bub3 complex is rapidly disassembled during mitotic slippage [13]. Using this readout, we assessed the ability of *glc7-10* cells to extinguish SAC signalling at kinetochores during slippage. To this end, we co-immunoprecipitated Mad1 with HA-tagged Bub3 from synchronised cells at different times of benomyl treatment. Despite the delayed slippage, the Bub3-Mad1 interaction was dismantled in *glc7-10* cells with kinetics similar to wild type cells (Figure 2A-B), suggesting that the delayed slippage upon PP1 inhibition is not accounted for by prolonged signalling at kinetochores.

We reasoned that PP1 could instead regulate the stability of the MCC. To look at MCC integrity, we checked by co-immunoprecipitation the amounts of HA-tagged Mad3 or Bub3, as well as Mad2, associated to myc-tagged Cdc20 in synchronized

wild type and *glc7-10* cells treated for various times with benomyl. While in wild type cells interaction of Mad3, Bub3 and Mad2 with Cdc20 declined after 4 hours of treatment when cells were still in mitosis, it was preserved in *glc7-10* cells (Figures 2C-D and S1A-B), suggesting that PP1 controls MCC stability during mitotic slippage. Since Cdc20 proteolysis is thought to contribute to MCC disassembly and SAC silencing [19,20], we wondered if Cdc20 degradation in mitosis, which requires Mad3 and the APC [21–24], could be affected by PP1 inactivation. However, kinetics of Cdc20 degradation were similar in wild type and *glc7-10* cells (Figure S1C), suggesting that they are not controlled by PP1. Interestingly, Mad3 phosphorylation was reproducibly increased in *glc7-10* versus wild type cells (Figures 2C and S1C), as assessed by its electrophoretic mobility, suggesting that PP1 might dephosphorylate Mad3.

MCC assembly does not require intact kinetochores [3,25]. Out of the SAC components that are part of the MCC, Mad3 is the only SAC protein that was not found enriched at kinetochores upon microtubule depolymerisation in budding yeast [26]. Our ChIP-on-chip analysis of the distribution of various SAC proteins along chromosome VI confirmed these observations: while Bub1, Bub3 and Mad1 were enriched around the centromere like the core kinetochore protein Ndc10 in nocodazole-arrested cells, Mad3 did not significantly concentrate at this chromosomal location (Figure 2E). The Mps1 kinase, which turns over rapidly at unattached kinetochores [27] could also be enriched at *CEN6*, albeit with lower efficiency than the aforementioned SAC proteins (Figure 2E). Thus, Mad3 might get incorporated mainly into soluble MCC, although we cannot rule out a possible fast

cycling (i.e. faster than Mps1) through unattached kinetochores. These results are consistent with the proposal that kinetochore recruitment of BubR1 (the metazoan counterpart of Mad3) is not essential to mount a SAC response [28,29]. Altogether, these data suggest that PP1 could promote mitotic slippage by controlling the stability of soluble MCC. Consistently, *MAD3* deletion could restore the ability of *glc7-10* cells to progress in the cell cycle upon *MAD2* overexpression, while deletion of Mad1, which is localised at kinetochores during SAC signalling and is not part of MCC [3,25,26], did not (Figure 2F). Furthermore, *MAD3* and *BUB3* deletion, but not deletion of *MAD1* and *BUB1*, could partially rescue the synthetic lethality of *GAL1-MAD2 glc7-10* cells on galactose-containing plates (Figure S1D).

We therefore conclude that PP1 controls mitotic slippage away from kinetochores.

PP1 promotes Mad3 dephosphorylation during mitotic slippage

Since the above results suggested that PP1 could control Mad3 dephosphorylation, we analysed the electrophoretic mobility of Mad3 during mitotic slippage on highly resolved gels and using TCA extracts, which preserve phosphorylations better than other protein extraction methods. Synchronised G1 cells were released in the presence of benomyl and at different times we analysed Mad3 phosphorylation state, as well as the levels of cell cycle markers, such as Cdc20, Clb2 and Sic1. After 4 hours from the release, Mad3 started being dephosphorylated in wild type cells but not in *glc7-10* cells (Figure. 3A), confirming the involvement of PP1 in this process. Mitotic slippage in the wild type was accompanied by Cdc20 and Clb2 degradation, albeit with different kinetics, as well as by Sic1 re-accumulation (Figure 3A-B).

Consistent with the idea that PP1 promotes mitotic slippage, Cdc20 and Clb2 remained stable in *glc7-10* cells for a longer time and no sign of Sic1 re-accumulation was detected during the time course.

PP1 is thought to reverse phosphorylations by Aurora B [30,31]. Since budding yeast Aurora B (Ipl1) phosphorylates Ser303 and Ser337 of Mad3 when kinetochore tension is absent [32], we reasoned that Ser303 and Ser337 dephosphorylation might be critical for mitotic slippage. Contrary to this prediction, mutating Ser303 and Ser337 to non-phosphorylatable alanines had a minor effect, if any, on the speed of mitotic slippage of wild type and *glc7-10* cells (Figure S2A-B).

To investigate if additional Mad3 phosphorylation sites would play a role in slippage, we immuno-purified Mad3 from wild type and *glc7-10* cells treated with benomyl for either 3 hours (when cells were arrested in mitosis) and 5 hours (when wild type cells were slipping out of mitosis) and searched for differential phosphorylation sites by mass spectrometry. Strikingly, a peptide phosphorylated on Ser268 in mitosis in both wild type and *glc7-10* cells became undetectable at 5 hours of benomyl treatment in wild type but not in *glc7-10* cells (Figure 3C-E), while the same unphosphorylated peptide was readily detected in all conditions (Figure S2C-E). Thus, Mad3 Ser268 could get dephosphorylated by PP1 during mitotic slippage. Since we were unsuccessful to generate specific antibodies against phospho-Ser268, we investigated if Ser268 phosphorylation could influence Mad3 electrophoretic mobility. Consistent with our previous data [37], Mad3 was heavily phosphorylated in mitosis; mutating Ser268 to Ala markedly reduced Mad3 mobility

shift in both wild type and *glc7-10* cells (Figure 3F), confirming that Ser268 is a major mitotic phosphorylation site and its dephosphorylation requires PP1. Ser268 is located 4 aminoacids after the first ABBA motif of Mad3 (Figure 3G) that is involved in MCC interaction with APC-Cdc20 [2,33,34]. Furthermore, Ser268 matches a loose consensus phosphorylation site for Polo kinase and Mps1 (E/D X S/T [35,36]). Mad3 is a known phosphorylation target of Polo and the Aurora B kinase Ipl1 [32,37], whereas no data so far addressed its possible phosphorylation by Mps1 in *S. cerevisiae*. Since Mps1 phosphorylates Mad3 in fission yeast [38], we asked if Mad3 phosphorylation depends on Mps1, in addition to the Polo kinase Cdc5. Remarkably, the electrophoretic mobility shift of Mad3 during mitosis of synchronised cells treated with nocodazole was markedly affected by inactivation of Mps1 and Cdc5 in an additive manner (Figure 3H), suggesting that both kinases contribute to Mad3 phosphorylation. Importantly, the impaired Mad3 phosphorylation in *mps1-1* mutant cells was not due to their inability to arrest mitotic progression upon nocodazole treatment, as a similar defect was observed by arresting cells in mitosis through APC inhibition by *CDC26* deletion (Figure S2F). Altogether, these data suggest that Mad3 Ser268 phosphorylation is antagonistically controlled by two kinases (Mps1 and Polo) and the PP1 phosphatase.

Ser268 of Mad3 is a critical PP1 target for mitotic slippage

To uncover the physiological relevance of Mad3 Ser268 dephosphorylation in mitotic slippage, we generated a non-phosphorylatable alanine mutant (*mad3-S268A*). The *mad3-S268A* mutation did not affect Mad3 protein stability (Figure S2G)

suggesting that it does not grossly alter protein folding. We then checked the influence of the *mad3-S268A* allele on the slippage kinetics of wild type and *glc7-10* cells synchronised in G1 and released in the presence of benomyl. Strikingly, the *mad3-S268A* allele advanced mitotic slippage in wild type cells under these conditions, as shown by the accelerated kinetics of Clb2 degradation, Sic1 re-accumulation and re-entry into the subsequent cell cycle (Figure 4A-B). Even more remarkably, it restored mitotic slippage in *glc7-10* cells (Figure 4A-B), indicating that Mad3 Ser268 is a critical PP1 target for mitotic slippage in budding yeast. Interestingly, *mad3-S268A* cells could activate the SAC as efficiently as wild type cells. Indeed, when released from a G1 arrest in the presence of nocodazole, which engages a stronger checkpoint response than benomyl [13], *mad3-S268A* and wild type cells arrested in mitosis for up to 5 hours with high levels of Clb2 and no rise in Sic1 levels, unlike *mad3Δ* cells that are SAC-deficient (Figure 4C-D). Furthermore, in the presence of sub-lethal doses of benomyl, *mad3-S268A* cells turned out to be only slightly more sensitive than wild type cells to the highest benomyl concentration tested (Figure 4E), supporting the idea that they are largely SAC-proficient.

We then investigated if the *mad3-S268A* mutation could have any impact on MCC assembly/stability. To this end, we tagged the *mad3-S268A* allele with 3HA epitopes and analysed its ability to co-immunoprecipitate Cdc20 and Mad2, using extracts from either cycling or nocodazole-treated cultures. Surprisingly, while Mad3 efficiently co-precipitated Cdc20 and Mad2, interaction of Mad3-S268 with these proteins was severely disrupted (Figure 4F). This result was confirmed in reciprocal experiments, where we immunoprecipitated myc18-Cdc20: while Cdc20 associated

efficiently with both Mad3 and Mad2 in nocodazole-treated wild type cells, it largely failed to pull down Mad3-S268A under the same conditions, despite its ability to associate normally with Mad2 (Figure 4G). We further investigated the impact of the *mad3-S268A* mutation on the interaction between Mad3 and Bub3, which form a stable dimer throughout the cell cycle [40], while under SAC-activating conditions they interact in the MCC [25]. Notably, immunoprecipitation of Bub3-myc18 from cycling cells pulled down HA-tagged Mad3 and Mad3-S268A with similar efficiency, while after nocodazole treatment Mad3-S268A was co-precipitated with Bub3 at lower levels than Mad3 (Figure S2H), suggesting that the *mad3-S268A* mutation affects mainly Bub3-Mad3 association within the MCC. Altogether, these data imply that Mad3 S268 phosphorylation, which is maximal in mitosis, stabilises the MCC, while its dephosphorylation by PP1 disrupts MCC integrity and allows slippage. Although its proximity to the ABBA1 motif would predict S268 to affect mostly the interaction between MCC and APC-Cdc20 [2], our data are consistent with the evidence that mutations in the ABBA1 motif of BubR1 somewhat impair MCC stability, besides MCC association with APC-Cdc20 [34]. Remarkably, E/D X S/T motifs can be found after the ABBA1 motif of Mad3/BubR1 from several organisms, suggesting a conserved regulatory function.

To reinforce the notion that Mad3 S268 phosphorylation stabilises the MCC, we attempted to generate a phosphomimetic *MAD3* variant by mutating S268 to glutamic acid (*mad3-S268E*). However, this mutant did not delay mitotic slippage (Figure S3A-B) and had an intermediate phenotype relative to wild type *MAD3* and *mad3-S268A*, in that it did not bypass the slippage delay of *glc7-10* cells (Figure S3C-

D) but somewhat destabilised the interaction of Mad3 with Cdc20 and Mad2, although not as severely as mad3-*S268A* (Figure S3E). Thus, the Mad3-S268E mutant protein does not behave as a phosphomimetic, which is not surprising given that it does not undergo the same mobility shift on SDS-page as naturally phosphorylated Mad3 (Figure S3E).

Although the overall phosphorylation of Mad3 requires both Polo kinase and Mps1, only Mps1 inactivation impaired the association of Mad2 and Mad3 with Cdc20 (Figure S3F) as previously shown [39], thus recapitulating the MCC destabilisation caused by the *mad3-S268A* mutation. On the basis of these results, we propose that Mps1 might be the prevailing kinase phosphorylating Mad3 Ser268 under checkpoint-activating conditions. In agreement with our data, Mps1-dependent phosphorylation of fission yeast Mad3 sustains a robust SAC response [38].

How can *mad3-S268A* cells be SAC-proficient in spite of their low MCC levels? We envision two non-exclusive explanations. The Mad3-S268A protein might be simply more dynamic than wild type Mad3 in the MCC, thereby failing to remain stably associated with other MCC components during our immunoprecipitation procedure. Another possibility is that Mad2 partially compensates for the low levels of MCC-bound Mad3 in APC-Cdc20 inhibition. Indeed, when Mad2 is artificially tethered to Cdc20, Mad3 becomes dispensable for APC inhibition, suggesting that an important physiological function of Mad3 could be to promote APC-Cdc20 inhibition by Mad2 [39]. We hypothesise that the ability of Mad2 to inhibit APC-Cdc20 activity might progressively fade during mitotic slippage, thus highlighting the importance of Mad3-S268 phosphorylation in holding a prolonged mitotic arrest. If this were the

case, altering MCC stoichiometry through an increase in Mad2 levels could restore normal kinetics of slippage in *mad3-S268A* cells. This was indeed the case. Upon *MAD2* overexpression, the *MAD3-S268A* allele did neither accelerate slippage in otherwise wild type or *glc7-10* cells (Figure S4A), nor did it suppress the synthetic lethality of *GAL1-MAD2 glc7-10* cells in the presence of galactose (Figure S4B-C). Similar results were obtained with the *mad3-S303,337A* or the *mad3-S268,303A,337A* alleles (Figure S4A-C). Thus, the *mad3-S268A* mutation could progressively weaken the ability of Mad2 to inhibit APC-Cdc20 upon prolonged SAC activation. Mad2 overexpression might provide a compensatory mechanism to overcome this defect. For instance, it could favour the formation of C-Mad2 over O-Mad2 [41], thereby stimulating MCC assembly and APC inhibition. It should be noticed, however, that the ability of *mad3-S268A* cells to impose a SAC-mediated mitotic arrest under physiological Mad2 levels suggests that at least another mechanism, besides Mad3 S268 dephosphorylation, promotes SAC silencing and APC-Cdc20 unleashing during slippage. We speculate that dephosphorylation of Mad2 and/or Cdc20 [42,43] could accompany this process.

Conclusions

Mitotic slippage is often considered as a passive process brought about by the gradual decline in cyclin B-CDK levels that allows mitotic exit below a critical threshold [5,44]. We propose that in budding yeast mitotic slippage is actively controlled and involves aspects of SAC silencing, such as MCC destabilisation aided by PP1-dependent Mad3 phosphorylation. Our data further imply that SAC silencing

by PP1 occurs not only at kinetochores, but also away from kinetochores, in agreement with recent observations in *Drosophila* [45]. Although the generality of these conclusions remains to be tested, it is tempting to speculate that different levels/activity of PP1 or other SAC-counteracting phosphatases could account for the highly variable duration of SAC-induced mitotic arrest in different species or upon treatment with different microtubule drugs [46,47]. Whether and how PP1 activity is controlled during prolonged SAC signalling is an important subject for future studies.

ACKNOWLEDGMENTS

We are grateful to E. Galati for initial experiments on the slippage defects of *glc7-10* mutant cells; to S. Ibanes for assistance with mass spec experiments; to A. Musacchio for structural analysis of Mad3-S268; to K. Hardwick, A. Hoyt, J. Kilmartin, K. Nasmyth, M. Stark, W. Zachariae for sharing reagents; to V. Georget for invaluable help with live cell imaging; to members of S. Piatti's lab for useful discussions. We acknowledge the imaging core facility MRI, member of the national infrastructure France-BioImaging supported by the French National Research Agency (ANR-10-INBS-04, "Investments for the future"). We acknowledge the Functional Proteomics Platform of Biocampus Montpellier where mass spectrometry experiments were carried out. This work has been supported by the Fondation pour la Recherche Médicale (DEQ20150331740 to S.P.).

AUTHOR CONTRIBUTIONS

Conceptualization, S.P. and A.R. ; Investigation, A.R., Y.K., M.S. and S.P. ; Data analysis, A.R. Y.K., K.S., M.S. and S.P. ; Figures, A.R. and S.P.; Writing, S.P. and A.R. with inputs from all authors ; Supervision, S.P. ; Project Administration, S.P. ; Funding acquisition, S.P.

DECLARATION OF INTERESTS

The authors declare no competing interests.

FIGURE LEGENDS

Figure 1. PP1 mutant cells are defective in mitotic slippage

(A-B): Wild-type (ySP7962) and *glc7-10* (ySP13457) cells were grown at 25°C, arrested in G1 with α-factor and released at 30°C in the presence of benomyl (t=0). α-factor (2 μg/ml) was re-added after 2 h to arrest cells in the next G1 phase after slippage. Samples were collected at the indicated times for Western blot analysis of Pds1-myc18, Clb2, Sic1 and Pgk1 (loading control) (A), as well as for DNA contents by FACS analysis (B). Note that after slippage cells undergo massive chromosome missegregation, mainly driven by astral microtubules that re-form with time during benomyl treatment [13].

(C): Serial dilutions of wild type (ySP41), *GAL1-MAD2* (ySP6170), *glc7-10* (ySP9304) and *GAL1-MAD2 glc7-10* (ySP13415) were spotted on YEPD (glucose) and YEPG (galactose) plates and incubated at 30°C. **(D):** The same strains as in (C) were grown in uninduced conditions (YEPR) at 25°C, arrested in G1 with α-factor and spotted on YEPG plates that were incubated at 30°C from the time of release (t=0). 200 cells were scored at each time point to determine the percentage of single cells (purple) and of microcolonies of two (green), four (red), or more than four cells (blue).
See also Video S1.

Figure 2. PP1 promotes slippage through disassembly of soluble MCC

(A-B): Wild-type (ySP14172) and *glc7-10* (ySP14222) cells expressing endogenously tagged Bub3-HA3 were grown at 25°C, arrested in G1 with α-factor

and released at 30°C in the presence of benomyl (t=0). Samples were collected at the indicated times to analyse the interaction of Bub3-HA3 with Mad1 by co-immunoprecipitations (A). Throughout the time course, DNA contents were measured by FACS analysis (B). Bub3 was immunoprecipitated with an anti-HA antibody and immunoprecipitates (IP) and inputs were probed by western blot with anti-HA and anti-Mad1 antibodies (A). As negative control (mock), nocodazole-arrested cells expressing untagged Bub3 (ySP41) were used. Inputs represent 1/50th of the extracts used for IPs. **(C-D):** Wild-type (ySP14905) and *glc7-10* mutant (ySP15043) expressing myc-tagged Cdc20 (myc18-Cdc20) and HA-tagged Mad3 (Mad3-HA3) were treated as in (A). Samples were collected at the indicated times to analyse the interaction between myc18-Cdc20 and Mad3-HA3 or Mad2 (C). At the same times, DNA contents were measured by FACS analysis (D). Myc18-Cdc20 was immunoprecipitated with an anti-myc antibody. Immunoprecipitates (IP) and inputs were probed by western blot with anti-HA, anti-Mad2 and anti-myc antibodies (C). As negative control (mock) benomyl arrested cells expressing untagged Cdc20 and Mad3-HA3 (ySP2220) were used. Inputs represent 1/50th of the extracts used for IPs. Clb2 was used as a mitotic marker. The amount of Mad3-HA3 and Mad2 co-immunoprecipitated with myc18-Cdc20 was quantified with ImageJ and plotted (graphs). **(E):** Cells expressing Ndc10-HA3 (ySP1333), Bub1-HA3 (ySP1593), Bub3-HA3 (ySP1346), Mad1-HA3 (ySP2216), Mps1-HA3 (ySP1923) or Mad3-HA3 (ySP2220) were arrested in mitosis by nocodazole treatment and the distribution of the tagged proteins on chromosome VI was analysed by ChIP and hybridization on a high-density oligonucleotide microarray. The dark grey peaks

represent significant enrichment of immunoprecipitated material. **(F):** wt (ySP41), *GAL1-MAD2* (ySP6170), *GAL1-MAD2 glc7-10* (ySP13415), *GAL1-MAD2 glc7-10 mad1Δ* (ySP14211) and *GAL1-MAD2 glc7-10 mad3Δ* (ySP14202) were grown in uninduced conditions (YEPR) at 25°C, arrested in G1 with α-factor and spotted on YEPG plates that were incubated at 30°C from the time of release (t=0) to allow microcolonies formation. 200 cells were scored at each time point to determine the percentage of single cells (purple) and of microcolonies of two (green), four (red), or more than four cells (blue).

See also Figure S1.

Figure 3. Mad3 is dephosphorylated by PP1 during mitotic slippage

(A-B): Wild-type (ySP2294) and *glc7-10* (ySP13792) cells expressing myc-tagged Cdc20 (myc18-Cdc20) and HA-tagged Mad3 (Mad3-HA3) were grown at 25°C, arrested in G1 with α-factor and released at 30°C in the presence of benomyl (t=0). Samples were collected at the indicated times for western blot analysis of myc18-Cdc20, Mad3-HA3, Clb2, Sic1, Mad2 and Pgk1 (loading control) (A). At the same time points, DNA contents were measured by FACS analysis (B). **(C-E):** MS/MS analysis of the Mad3 phospho-peptide NNVFVDGEEpS^{268}DVELFETPNR (extracted by precursor ion M at m/z 1195,5128 ++). The Isotope Dot Product (idotp) allows to assess the distribution of the precursor isotope and its correlation between expected and observed pattern, with optimal matching resulting in an idotp value =1 (C). The skyline (D) displays a library of MS/MS spectra for the selected peptide that provides underlying peptide identification information for a specific condition (in

this case *glc7-10* at 5hrs of benomyl treatment. Chromatograms and peak intensity traces for the four samples (wt 3hrs, wt 5 hrs, *glc7-10* 3hrs and *glc7-10* 5hrs) are displayed (E). The extracted ion chromatograms for isotope peaks at m/z 1195,5128 are displayed for each condition after MS1 filtering for peptide NNVFVDGEEpS^{268}DVELFETPNR. The vertical lines with annotated retention times and identification (ID) mark underlying MS/MS sampling that initially directed MS1 peak picking. **(F):** Wild-type (ySP2220), *glc7-10* (ySP13548), *mad3-S268A* (ySP15081) and *glc7-10 mad3-S268A* (ySP15072) cells all expressing Mad3-HA3 were grown at 25°C, arrested in G1 with α-factor and released at 30°C in the presence of nocodazole (t=0). Samples were collected at the indicated times for western blot analysis of Mad3 with an anti-HA antibody. **(G):** Schematic view of the Mad3 protein, highlighting the two KEN boxes, the TPR region, the two ABBA domains and S268. **(H):** Wild-type (ySP2220), *mps1-1* (ySP2263), *cdc5-2* (ySP2514), *mps1-1 cdc5-2* (ySP3497) and *mad3-S268A* (ySP14967) cells all carrying HA-tagged Mad3 were treated as in (F), except that cells were released from the G1 arrest at 37°C. Clb2 was used as a mitotic marker in the western blot.
See also Figure S2.

Figure 4. Mad3 S268 dephosphorylation facilitates mitotic slippage

(A-B): Wild-type (ySP1056), *glc7-10* (ySP14763), *mad3-S268A (*ySP14774) and *glc7-10 mad3-S268A (*ySP14775*)* cells were grown at 25°C, arrested in G1 with α-factor and released at 30°C in the presence of benomyl (t=0). α-factor (2 μg/ml) was re-added after 2h to arrest cells in the next G1 phase after slippage. Samples were

collected at the indicated times for Western blot analysis of Clb2, Sic1 and Pgk1 (loading control) (A), as well as for FACS analysis of DNA contents (B). **(C-D):** Wild-type (ySP1056), *mad3Δ* (ySP14837) and *mad3-S268A* (ySP14774) cells were grown at 25°C, arrested in G1 with α-factor and released in the presence of nocodazole (t=0). Samples were collected at the indicated times for Western blot analysis of Clb2, Sic1 and Pgk1 (loading control) (C) and for FACS analysis of DNA contents (D). **(E):** Serial dilutions of wild type (ySP41), *mad3Δ* (ySP1577) and *mad3-S268A* (ySP14070) cells were spotted on YEPD without or with the indicated concentration of benomyl (ben) and incubated at 30°C. **(F-G):** Cycling cultures (cyc) of wild type (ySP2294) and *mad3-S268A* mutant cells (ySP14966) expressing myc-tagged Cdc20 (myc18-Cdc20) and HA-tagged Mad3 (Mad3-HA3), were treated with nocodazole (noc) at 25°C for 3h. As negative controls (mock), cycling and nocodazole-arrested cells expressing either Mad3HA3 (ySP2220, F) or myc18-Cdc20 (ySP1414, G) were used. Mad3 was immunoprecipitated from the extracts with anti-HA antibodies (F), whereas Cdc20 was immunoprecipitated with anti-myc antibodies (G). Immunoprecipitates (IP) along with the Inputs ($1/50^{th}$ of the extracts used for IPs), were immunoblotted with anti-HA, anti-myc and anti-Mad2 antibodies.
See also Figure S2, S3, S4.

STAR Methods

Lead Contact and Materials Availability

Additional information or requests for resources and reagents can be directed to and will be fulfilled by the Lead Contact, Simonetta Piatti (simonetta.piatti@crbm.cnrs.fr). Yeast strains generated in this study have not been deposited on an external repository but are available for distribution on request from the Lead Contact.

Strains and growth conditions

All yeast strains (Key Resources Table) are congenic or at least four times backcrossed to W303 (ySP41 : *ade2-1*, *trp1-1*, *leu2-3,112*, *his3-11*, and *15 ura3*). The *GAL1-MAD2* construct and its integration at the *URA3* locus has been previously described [13]. The *myc18-CDC20, mad3::K.l.TRP1* and *bub1::S.p.HIS5* strains were kindly provided by K. Nasmyth [48,49]. One-step tagging techniques [50] were used to create strains expressing C-terminally tagged proteins (Bub1-HA3, Bub3-HA3, Mad1-HA3, Mad3-HA3 and Mad3-6Gly-3Flag) from their respective genomic loci. To generate the *NDC10-HA3* strain (ySP1333), an HA3 NotI cassette was introduced in a pRS304 plasmid bearing the NdeI/XbaI 1170 bp fragment of *NDC10* (part of CDS and 3'UTR) and carrying a NotI site before the stop codon (a kind gift from J. Kilmartin). The resulting plasmid (pSP62) was cut with BclI for integration at the *NDC10* locus. This generates a full length copy of HA-tagged *NDC10* and a truncated duplication of *NDC10*. The *glc7-10* mutant was kindly provided by M. Stark [51]. The

bub3::LEU2 deletion was a kind gift from A. Hoyt [52]. *MAD3* mutant plasmids (Key Resources Table) were created by replacing part of the *MAD3* coding region (from the BglII site at position 703 to the XbaI site at position 1162 from the ATG) with synthetic *MAD3* DNA fragments (MWG Eurofins) in a Yiplac128-derived plasmid (pSP1395) that contained the *MAD3* CDS comprising 474 bp of 5' UTR and 200 bp of 3' UTR cloned as an EcoRI DNA fragment that was amplified by PCR from the genomic DNA of ySP41 with primers SP299 and SP329. Integration of the *MAD3* mutant plasmids was directed to the *LEU2* locus by AflII digestion. Single copy integration was verified by Southern blot.

Yeast cultures were grown at 25–30°C in YEP (1% yeast extract, 2% bactopeptone, 50 mg/l adenine) medium supplemented with 2% glucose (YEPD), 2% raffinose (YEPR), 2% galactose (YEPG) or 2% raffinose and 1% galactose (YEPRG). Unless otherwise stated, α-factor was used at 4μg/ml for *BAR1* and 0.2 μg/ml for *bar1* strains. G1 arrest was monitored under a transmitted light microscope and cells were released in fresh medium (typically after 120–135 min of alpha factor treatment) after being collected by centrifugation at 2000*g* and washed with YEP containing the appropriate sugar. For galactose induction of α-factor–synchronized cells, galactose was added 30 min before release. Nocodazole was used at 15 μg/ml. Benomyl was used at 10, 12.5 or 15 μg/ml in YEPD to test the sensitivity of strains on plates or at 80 μg/ml for mitotic slippage experiments.

Microcolony Assay

Yeast cultures were grown overnight at 25°C in YEPR. Cells were syncronized with α-factor and 1% galactose was added 30 min before release. Cells were collected and washed with YEPRG two times and spotted on YEPG plates at 30° (t = 0). At various times after release, 200 cells for each strain were scored to determine the frequency of single cells and of microcolonies of two, four, or more than four cells.

Protein extracts, immunoprecipitations and western blotting

For TCA protein extracts, 10–15 ml of cell culture in logarithmic phase (OD_{600} = 05-1) were collected by centrifugation at 2000*g*, washed with 1 ml of 20% TCA and resuspended in 100 µl of 20% TCA before breakage of cells with glass beads (diameter 0.5–0.75 mm) on a Vibrax VXR (IKA). After addition of 400 µl of 5% TCA, lysates were centrifuged for 10 min at 845 *g*. Protein precipitates were resuspended in 100 µl of 3× SDS sample buffer (240 mM Tris-Cl pH6.8, 6% SDS, 30% glycerol, 2.28 M β-mercaptoethanol, 0.06% bromophenol blue), denatured at 99 °C for 3 min and loaded on SDS-PAGE after elimination of cellular debris by centrifugation (5 min at 20,000*g*).

To resolve Mad3 phosphorylation forms, denatured protein samples were loaded on 20 x 20 cm 12.5% gels and run until the bromophenol blue of the sample buffer migrated ~3cm from the bottom of the gel.

For immunoprecipitations, cells were lysed with glass beads in IP buffer (20% glycerol, 150 mM NaCl , 50 mM Hepes pH 7.4, 1mM EDTA, 1 mM sodium orthovanadate, 60 mM β-glycerophosphate, supplemented with a cocktail of protease inhibitors (2X Complete; Roche) at 4°C with 14 cycles of 30" breakage

followed by 30" in ice. 6 ODs of cleared extracts were diluted with IP buffer in 500 µl, out of which 10 µl were withdrawn and denatured in 3 x SDS sample buffer for inputs. The remaining IP extract was incubated for 1h with 50 µl of protein A–Sepharose (slurry 1:1 in IP buffer) that had been pre-adsorbed with 1 µl of anti-HA (12CA5) or anti-myc (9E10) antibody for 90' at 4°C with shaking. The slurry was washed four times with IP buffer and twice with PBS before loading on SDS page gels.

Proteins were wet-transferred to Protran membranes (Schleicher and Schuell) overnight at 0.2 A and probed with anti-myc 9E10 mAb (1:5000), anti-HA 12CA5 mAb (1:5000), sheep polyclonal antibodies against Mad2 (a generous gift from K. Hardwick , 1:1000), monoclonal anti-Pgk1 (1:40000, Invitrogen), polyclonal anti-Sic1 (1:200, Santa Cruz) or polyclonal anti-Clb2 (a generous gift from W. Zachariae, 1:2000, or from Santa Cruz, 1:1000). Antibodies were diluted in 5% low-fat milk (Regilait). Secondary antibodies were purchased from GE Healthcare and diluted according to the manufacturer. Proteins were detected by a home-made enhanced chemiluminescence system.

FACS analysis of DNA contents

For flow cytometric DNA quantification, 5×10^6–2×10^7 cells were collected at each time point, spun at 10,000*g* and fixed with 1 ml of 70% ethanol for at least 30 min at RT. After one wash with 50 mM Tris-Cl pH 7.5, cells were resuspended in 0.5 ml of the same buffer containing 0.025 ml of a preboiled 10 mg/ml RNAse solution and incubated overnight at 37 °C. The next day cells were spun at 10,000*g* and

resuspended in 0.5 ml of 5 mg/ml pepsin freshly diluted in in 55 mM HCl. After 30 min incubation at 37 °C cells were washed with FACS buffer (200 mM Tris-Cl pH 7.5, 200 mM NaCl, 78 mM $MgCl_2$) and resuspended in the same buffer containing 50 μg/ml propidium iodide. After a short sonication samples were diluted (1:20–1:100) in 1 ml of 50 mM Tris-Cl pH 7.5 and analyzed with a FACSCalibur device (BD Biosciences). Totally, 10,000 events were scored for each sample and plotted after gating out the debris.

MS/MS analysis

Sample preparation

6Gly-3FLAG-tagged Mad3 was purified from wt and *glc7-10* cells as follows. About 10^{10} cells treated with 80 μg/ml benomyl for 3h or 5h were harvested by centrifugation at 4000*g* for 10' at 4°C and washed with 25 ml of cold 10mM Tris-Cl pH 7.5. Cell pellets were snap frozen in liquid N_2 and stored at -80°C. Cells were thawn 10' in ice and washed with 15 ml of filtered TBSN (25mM Tris-Cl pH 7.4, 100mM NaCl, 2mM EDTA, 0,1% Igipal, 1mM DTT) before being resuspended in 8 ml of TBSN supplemented with a cocktail of protease and phosphatase inhibitors (Complete EDTA-free cocktails tablets Roche (2X), PhosSTOP Roche (2X) and 1mM PMSF (Sigma)). Cell breakage was performed in dry ice with glass beads (diameter 0.5–0.75 mm) using a FastPrep bead beater (MP Biomedicals) with 5 cycles of 20s shaking at 4m/s speed with 5' of pause between cycles. Lysates (8-9 ml) were cleared by ultracentrifugation in a 90Ti rotor (Beckman) at 50000 rpm for 1h at 4°C. Cleared extracts were incubated with 150μl of Protein G-dynabeads previously

crosslinked with 30 µl of FLAG M2 antibody (Sigma) on a rotating wheel for 1h at 4°C. Dynabeads were washed four times with TBSN buffer and twice with cold PBS (shaking for 10min at 4°C on a nutator during each wash) before adding 100 µl of elution buffer (50mM Tris-Cl pH 8.3, 1mM EDTA, 0,1% SDS) supplemented with 0,5 mg/mL of 3xFLAG peptide. The slurry was swirled on a thermomixer (800rpm) at RT for 25min. Finally, eluted proteins were separated from the beads and frozen at -80°C . Eluates were run on a 4–15% precast Mini-Protean TGX gel (Bio-Rad) and stained with Coomassie blue. Lanes were cut in small gel pieces and in-gel trypsin digestion was performed as described [53].

High-performance liquid chromatography and MS measurements

The generated peptides were loaded onto a 15 cm reversed phase column (75 mm inner diameter, Acclaim Pepmap 100® C18, Thermo Fisher Scientific) with an Ultimate 3000 RSLC system (Thermo Fisher Scientific) directly coupled online to the MS (Q Exactive Plus, Thermo Fisher Scientific) via a nano-electrospray source. Peptides were introduced onto the column with buffer A (0.1% formic acid) and eluted with a 103-min gradient of 5 to 40% of buffer B (80% ACN, 0.1% formic acid) at a flow rate of 300 nl/min.

The mass spectrometer was programmed to acquire in a data-dependent mode. Full scans (375 – 1,500 m/z) were acquired in the Orbitrap mass analyzer with resolution 70,000 at 200 m/z. For the full scans, 3E6 ions were accumulated within a maximum injection time of 60 ms and detected in the Orbitrap analyzer. The twelve most intense ions with charge states ≥ 2 were sequentially isolated to a target value of 1e5 with a maximum injection time of 45 ms and fragmented by HCD

in the collision cell (normalized collision energy of 28%) and detected in the Orbitrap analyzer at 17,500 resolution.

Bioinformatic analysis

Raw mass spectrometric data was analyzed in the MaxQuant environment, versions 1.5.5.1, and employing Andromeda for database search with label-free quantification (LFQ), match between runs and the iBAQ algorithm enabled [54]. The MS/MS spectra were matched against the UniProt Reference proteome (Proteome ID UP000002311) of *S. cerevisiae* (strain ATCC 204508 / S288c) (release 2018_04; http://www.uniprot.org) and 270 frequently observed contaminants as well as reversed sequences of all entries. The following settings were applied: spectra were searched with a mass tolerance of 7 ppm (MS) and 0.5 Th (MS/MS). Enzyme specificity was set to trypsin/P, and the search included cysteine carbamidomethylation as a fixed modification and oxidation of methionine, acetylation (protein N-term) and/or phosphorylation of Ser, Thr, Tyr residue (STY) as variable modifications. Up to two missed cleavages were allowed for protease digestion. FDR was set at 0.01 for peptides and proteins and the minimal peptide length at 7.

The MaxQuant software generates several output files that contain information about identified peptides and proteins. The “proteinGroups.txt” file is dedicated to identified proteins: each single row collapses into protein groups all proteins that cannot be distinguished based on identified proteins. An in-house bioinformatics tool (leading v3.2) has been developed to automatically select a representative protein ID in each protein group. First, proteins with the most identified peptides

are isolated in a so called “match group” (proteins from the “Protein IDs” column with the maximum number of “peptides counts (all)”). For the remaining match groups where more than one protein ID existed after filtering, the “leading” protein has been chosen as the best annotated protein in UniProtKB (reviewed entries rather than automatic ones, the one with the highest protein existence evidence). XIC *(*Extracted Ion Chromatogram), XIC filtering and peak detection to certain Mad3 peptides (NNVFVDGEESDVELFETPNR and NNVFVDGEE**pS**^{268}DVELFETPNR) were performed using the Skyline software v4.1.0.11717 [55]. Total areas were used for ion intensity integration of peptides (Figures 3C,E and S2C,D).

Microscopy

For time-lapse video microscopy cells were mounted on 1% agarose pads in YEPRG medium in a four-compartment fluorodish, filmed at 30°C with a 100X Plan Apochromat 1.40NA oil immersion objective mounted on an Epifluorescence Nikon Ti2 inverted microscope coupled to a CMOS back-illuminated Prime95B Photometrics camera controlled by the NIS Element software. Cells were filmed every 2’ for 12 hours.

Data and Code Availability

This paper did not generate any datasets or new code. All raw data is available upon request.

SUPPLEMENTAL MATERIAL

Video S1. PP1 mutant cells are defective in mitotic slippage. Related to Figure 1.

The same strains as in Figure 1C were grown in YEPR at 25°C, arrested in G1 by α-factor and then released in YEPRG at 30°C in a four-compartment fluorodish. Cells were filmed every 2' for 12 hours. Scale bar: 5 μm.

REFERENCES

1. Musacchio, A. (2015). The Molecular Biology of Spindle Assembly Checkpoint Signaling Dynamics. Curr. Biol. *25*, R1002–R1018.
2. Alfieri, C., Chang, L., Zhang, Z., Yang, J., Maslen, S., Skehel, M., and Barford, D. (2016). Molecular basis of APC/C regulation by the spindle assembly checkpoint. Nature *536*, 431–436.
3. Sudakin, V., Chan, G.K., and Yen, T.J. (2001). Checkpoint inhibition of the APC/C in HeLa cells is mediated by a complex of BUBR1, BUB3, CDC20, and MAD2. J. Cell Biol. *154*, 925–36.
4. Rieder, C.L., and Maiato, H. (2004). Stuck in division or passing through: what happens when cells cannot satisfy the spindle assembly checkpoint. Dev. Cell *7*, 637–51.
5. Brito, D.A., and Rieder, C.L. (2006). Mitotic checkpoint slippage in humans occurs via cyclin B destruction in the presence of an active checkpoint. Curr. Biol. *16*, 1194–200.
6. Bonaiuti, P., Chiroli, E., Gross, F., Corno, A., Vernieri, C., Štefl, M., Cosentino Lagomarsino, M., Knop, M., and Ciliberto, A. (2018). Cells Escape an Operational Mitotic Checkpoint through a Stochastic Process. Curr. Biol. *28*, 28-37.
7. Pinsky, B.A., Nelson, C.R., and Biggins, S. (2009). Protein Phosphatase 1 Regulates Exit from the Spindle Checkpoint in Budding Yeast. Curr. Biol. *19*, 1182-1187.
8. Vanoosthuyse, V., and Hardwick, K.G. (2009). A Novel Protein Phosphatase 1-Dependent Spindle Checkpoint Silencing Mechanism. Curr. Biol. *19*, 1176-1181.
9. Meadows, J.C., Shepperd, L.A., Vanoosthuyse, V., Lancaster, T.C., Sochaj, A.M., Buttrick, G.J., Hardwick, K.G., and Millar, J.B.A. (2011). Spindle checkpoint silencing requires association of PP1 to both Spc7 and kinesin-8 motors. Dev. Cell *20*, 739–750.
10. London, N., Ceto, S., Ranish, J.A., and Biggins, S. (2012). Phosphoregulation of Spc105 by Mps1 and PP1 Regulates Bub1 Localization to Kinetochores. Curr. Biol. *22*, 900–906.
11. Rosenberg, J.S., Cross, F.R., and Funabiki, H. (2011). KNL1/Spc105 recruits PP1 to silence the spindle assembly checkpoint. Curr. Biol. *21*, 942–947.
12. Rieder, C.L., and Maiato, H. (2004). Stuck in division or passing through: what happens when cells cannot satisfy the spindle assembly checkpoint. Dev. Cell *7*, 637–51.
13. Rossio, V., Galati, E., Ferrari, M., Pellicioli, A., Sutani, T., Shirahige, K., Lucchini, G., and Piatti, S. (2010). The RSC chromatin-remodeling complex influences mitotic exit and adaptation to the spindle assembly checkpoint by controlling the Cdc14 phosphatase. J. Cell Biol. *191*, 981–97.
14. Schwob, E., Bohm, T., Mendenhall, M.D., and Nasmyth, K. (1994). The B-type cyclin kinase inhibitor p40SIC1 controls the G1 to S transition in S. cerevisiae [see comments] [published erratum appears in Cell 1996 Jan 12;84(1):following 174]. Cell *79*, 233–44.
15. London, N., and Biggins, S. (2014). Mad1 kinetochore recruitment by Mps1-mediated phosphorylation of Bub1 signals the spindle checkpoint. Genes Dev. *28*,

140–152.
16. Shepperd, L.A., Meadows, J.C., Sochaj, A.M., Lancaster, T.C., Zou, J., Buttrick, G.J., Rappsilber, J., Hardwick, K.G., and Millar, J.B.A. (2012). Phosphodependent recruitment of Bub1 and Bub3 to Spc7/KNL1 by Mph1 kinase maintains the spindle checkpoint. Curr. Biol. *22*, 891–899.
17. Primorac, I., Weir, J.R., Chiroli, E., Gross, F., Hoffmann, I., van Gerwen, S., Ciliberto, A., and Musacchio, A. (2013). Bub3 reads phosphorylated MELT repeats to promote spindle assembly checkpoint signaling. eLife *2*, e01030.
18. Yamagishi, Y., Yang, C.-H., Tanno, Y., and Watanabe, Y. (2012). MPS1/Mph1 phosphorylates the kinetochore protein KNL1/Spc7 to recruit SAC components. Nat. Cell Biol. *14*, 746–752.
19. Foster, S.A., and Morgan, D.O. (2012). The APC/C subunit Mnd2/Apc15 promotes Cdc20 autoubiquitination and spindle assembly checkpoint inactivation. Mol. Cell *47*, 921–932.
20. Mansfeld, J., Collin, P., Collins, M.O., Choudhary, J.S., and Pines, J. (2011). APC15 drives the turnover of MCC-CDC20 to make the spindle assembly checkpoint responsive to kinetochore attachment. Nat. Cell Biol. *13*, 1234–1243.
21. Pan, J., and Chen, R.-H. (2004). Spindle checkpoint regulates Cdc20p stability in Saccharomyces cerevisiae. Genes Dev. *18*, 1439–1451.
22. Prinz, S., Hwang, E.S., Visintin, R., and Amon, A. (1998). The regulation of Cdc20 proteolysis reveals a role for APC components Cdc23 and Cdc27 during S phase and early mitosis. Curr. Biol. *8*, 750–60.
23. Foe, I.T., Foster, S.A., Cheung, S.K., DeLuca, S.Z., Morgan, D.O., and Toczyski, D.P. (2011). Ubiquitination of Cdc20 by the APC occurs through an intramolecular mechanism. Curr. Biol. *21*, 1870–1877.
24. King, E.M., van der Sar, S.J., and Hardwick, K.G. (2007). Mad3 KEN Boxes Mediate both Cdc20 and Mad3 Turnover, and Are Critical for the Spindle Checkpoint. PLoS ONE *2*, e342.
25. Fraschini, R., Beretta, A., Sironi, L., Musacchio, A., Lucchini, G., and Piatti, S. (2001). Bub3 interaction with Mad2, Mad3 and Cdc20 is mediated by WD40 repeats and does not require intact kinetochores. EMBO J. *20*, 6648–59.
26. Gillett, E.S., Espelin, C.W., and Sorger, P.K. (2004). Spindle checkpoint proteins and chromosome-microtubule attachment in budding yeast. J. Cell Biol. *164*, 535–46.
27. Howell, B.J., Moree, B., Farrar, E.M., Stewart, S., Fang, G., and Salmon, E.D. (2004). Spindle Checkpoint Protein Dynamics at Kinetochores in Living Cells. Curr. Biol. *14*, 953–964.
28. Kulukian, A., Han, J.S., and Cleveland, D.W. (2009). Unattached Kinetochores Catalyze Production of an Anaphase Inhibitor that Requires a Mad2 Template to Prime Cdc20 for BubR1 Binding. Dev. Cell *16*, 105–117.
29. Malureanu, L.A., Jeganathan, K.B., Hamada, M., Wasilewski, L., Davenport, J., and van Deursen, J.M. (2009). BubR1 N Terminus Acts as a Soluble Inhibitor of Cyclin B Degradation by APC/CCdc20 in Interphase. Dev. Cell *16*, 118–131.
30. Francisco, L., Wang, W., and Chan, C.S. (1994). Type 1 protein phosphatase acts in opposition to IpL1 protein kinase in regulating yeast chromosome segregation. Mol. Cell. Biol. *14*, 4731–4740.

31. Hsu, J.Y., Sun, Z.W., Li, X., Reuben, M., Tatchell, K., Bishop, D.K., Grushcow, J.M., Brame, C.J., Caldwell, J.A., Hunt, D.F., *et al.* (2000). Mitotic phosphorylation of histone H3 is governed by Ipl1/aurora kinase and Glc7/PP1 phosphatase in budding yeast and nematodes. Cell *102*, 279–291.
32. King, E.M.J., Rachidi, N., Morrice, N., Hardwick, K.G., and Stark, M.J.R. (2007). Ipl1p-dependent phosphorylation of Mad3p is required for the spindle checkpoint response to lack of tension at kinetochores. Genes Dev. *21*, 1163–1168.
33. Rancati, G., Crispo, V., Lucchini, G., and Piatti, S. (2005). Mad3/BubR1 phosphorylation during spindle checkpoint activation depends on both Polo and Aurora kinases in budding yeast. Cell Cycle *4*, 972–80.
34. Di Fiore, B., Davey, N.E., Hagting, A., Izawa, D., Mansfeld, J., Gibson, T.J., and Pines, J. (2015). The ABBA Motif Binds APC/C Activators and Is Shared by APC/C Substrates and Regulators. Dev. Cell *32*, 358–372.
35. Di Fiore, B., Wurzenberger, C., Davey, N.E., and Pines, J. (2016). The Mitotic Checkpoint Complex Requires an Evolutionary Conserved Cassette to Bind and Inhibit Active APC/C. Mol. Cell *64*, 1144–1153.
36. Dou, Z., von Schubert, C., Körner, R., Santamaria, A., Elowe, S., and Nigg, E.A. (2011). Quantitative Mass Spectrometry Analysis Reveals Similar Substrate Consensus Motif for Human Mps1 Kinase and Plk1. PLoS ONE *6*, e18793.
37. Nakajima, H., Toyoshima-Morimoto, F., Taniguchi, E., and Nishida, E. (2003). Identification of a consensus motif for Plk (Polo-like kinase) phosphorylation reveals Myt1 as a Plk1 substrate. J Biol. Chem. *278*, 25277–80.
38. Zich, J., May, K., Paraskevopoulos, K., Sen, O., Syred, H.M., van der Sar, S., Patel, H., Moresco, J.J., Sarkeshik, A., Yates, J.R., *et al.* (2016). Mps1Mph1 Kinase Phosphorylates Mad3 to Inhibit Cdc20Slp1-APC/C and Maintain Spindle Checkpoint Arrests. PLOS Genetics *12*, e1005834.
39. Hardwick, K.G., Johnston, R.C., Smith, D.L., and Murray, A.W. (2000). MAD3 encodes a novel component of the spindle checkpoint which interacts with Bub3p, Cdc20p, and Mad2p. J. Cell Biol. *148*, 871–82.
40. Lau, D.T.C., and Murray, A.W. (2012). Mad2 and Mad3 Cooperate to Arrest Budding Yeast in Mitosis. Curr. Biol. *22*, 180–190.
41. De Antoni, A., Pearson, C.G., Cimini, D., Canman, J.C., Sala, V., Nezi, L., Mapelli, M., Sironi, L., Faretta, M., Salmon, E.D., *et al.* (2005). The Mad1/Mad2 Complex as a Template for Mad2 Activation in the Spindle Assembly Checkpoint. Curr. Biol. *15*, 214–225.
42. Tang, Z., Shu, H., Oncel, D., Chen, S., and Yu, H. (2004). Phosphorylation of Cdc20 by Bub1 provides a catalytic mechanism for APC/C inhibition by the spindle checkpoint. Mol. Cell *16*, 387–97.
43. Zich, J., Sochaj, A.M., Syred, H.M., Milne, L., Cook, A.G., Ohkura, H., Rappsilber, J., and Hardwick, K.G. (2012). Kinase activity of fission yeast Mph1 is required for Mad2 and Mad3 to stably bind the anaphase promoting complex. Curr. Biol. *22*, 296–301.
44. Gascoigne, K.E., and Taylor, S.S. (2008). Cancer cells display profound intra- and interline variation following prolonged exposure to antimitotic drugs. Cancer Cell *14*, 111–22.

45. Moura, M., Osswald, M., Leça, N., Barbosa, J., Pereira, A.J., Maiato, H., Sunkel, C.E., and Conde, C. (2017). Protein Phosphatase 1 inactivates Mps1 to ensure efficient Spindle Assembly Checkpoint silencing. eLife *6*, e25366.
46. Collin, P., Nashchekina, O., Walker, R., and Pines, J. (2013). The spindle assembly checkpoint works like a rheostat rather than a toggle switch. Nat. Cell Biol. *15*, 1378–1385.
47. Komaki, S., and Schnittger, A. (2017). The Spindle Assembly Checkpoint in Arabidopsis Is Rapidly Shut Off during Severe Stress. Dev. Cell *43*, 172-185.e5.
48. Shirayama, M., Zachariae, W., Ciosk, R., and Nasmyth, K. (1998). The Polo-like kinase Cdc5p and the WD-repeat protein Cdc20p/fizzy are regulators and substrates of the anaphase promoting complex in Saccharomyces cerevisiae. EMBO J. *17*, 1336–49.
49. Alexandru, G., Zachariae, W., Schleiffer, A., and Nasmyth, K. (1999). Sister chromatid separation and chromosome re-duplication are regulated by different mechanisms in response to spindle damage. EMBO J. *18*, 2707–21.
50. Janke, C., Magiera, M.M., Rathfelder, N., Taxis, C., Reber, S., Maekawa, H., Moreno-Borchart, A., Doenges, G., Schwob, E., Schiebel, E., *et al.* (2004). A versatile toolbox for PCR-based tagging of yeast genes: new fluorescent proteins, more markers and promoter substitution cassettes. Yeast *21*, 947–62.
51. Andrews, P.D., and Stark, M.J. (2000). Type 1 protein phosphatase is required for maintenance of cell wall integrity, morphogenesis and cell cycle progression in Saccharomyces cerevisiae. J. Cell. Sci. *113*, 507–520.
52. Hoyt, M.A., Totis, L., and Roberts, B.T. (1991). S. cerevisiae genes required for cell cycle arrest in response to loss of microtubule function. Cell *66*, 507–17.
53. Sun, W., Gao, S., Wang, L., Chen, Y., Wu, S., Wang, X., Zheng, D., and Gao, Y. (2006). Microwave-assisted protein preparation and enzymatic digestion in proteomics. Mol. Cell. Proteomics *5*, 769–776.
54. Cox, J., and Mann, M. (2008). MaxQuant enables high peptide identification rates, individualized p.p.b.-range mass accuracies and proteome-wide protein quantification. Nat. Biotechnol. *26*, 1367–1372.
55. Schilling, B., Rardin, M.J., MacLean, B.X., Zawadzka, A.M., Frewen, B.E., Cusack, M.P., Sorensen, D.J., Bereman, M.S., Jing, E., Wu, C.C., *et al.* (2012). Platform-independent and Label-free Quantitation of Proteomic Data Using MS1 Extracted Ion Chromatograms in Skyline: APPLICATION TO PROTEIN ACETYLATION AND PHOSPHORYLATION. Mol. Cell. Proteomics *11*, 202–214.

KEY RESOURCES TABLE

REAGENT or RESOURCE	SOURCE	IDENTIFIER
Antibodies		
Anti-myc 9E10 mAb	In house made (this paper)	
Anti-HA 12CA5	In house made (this paper)	
Anti-Flag	Sigma-Aldrich Cat# F3165	RRID:AB_259529
Anti-Mad2	K. Hardwick [39]	
Anti-Pgk1	Thermo Fisher Scientific Cat# 459250	RRID:AB_2532235
Anti-Sic1 (FL-284)	Santa Cruz Biotechnology Cat# sc-50441	RRID:AB_785671
Anti-Clb2	Santa Cruz Biotechnology Cat# sc-9071	RRID:AB_667962
Chemicals, Peptides, and Recombinant Proteins		
Agar	Formedium Cat# AGA03	
D(+)-Galactose	Formedium Cat# GAL03	
D(+)-Glucose anydrous	Formedium Cat# GLU03	
Peptone	Formedium Cat# PEP03	
D(+)-Raffinose pentahydrate	Formedium Cat# RAF04	
Yeast extract	Formedium Cat# YEA03	
Nocodazole	USBiological Cat# N3000	
Methyl 1-(butylcarbamoyl)-2-benzimidazolecarbamate (Benomyl)	Merck Cat# 381586	
α-factor	GenScript Cat# RP01002	
3X Flag peptide	GenScript (this paper)	
Protein A sepharose CL-4B	GE Healthcare Cat# 17078001	
Protein G dynabeads	Invitrogen Cat# 10003D	
Deposited Data		
Saccharomyces genome database		https://www.yeastgenome.org/
UniProt Reference proteome of *S. cerevisiae*	ATCC 204508 / S288c	http://www.uniprot.org
Experimental Models: Organisms/Strains		
S. cerevisiae: Strain background: W303	ATCC	ATTC: 208353
MATa, bar1::kanMX4	Lab stock	ySP1056

MATa, NDC10-HA3::TRP1	Lab stock	ySP1333
MATa, BUB3-HA3::K.l.URA3	Lab stock	ySP1346
MATα, myc18-CDC20::TRP1	Lab stock	ySP1414
MATa, mad3::K.l.TRP1	Lab stock	ySP1577
MATa, BUB1-HA3::K.l.URA3	Lab stock	ySP1593
MATa, MPS1-HA3::K.l.URA3	Lab stock	ySP1923
MATa, MAD1-HA3::K.l.URA3	Lab stock	ySP2216
MATa, MAD3-HA3::K.l.URA3	Lab stock	ySP2220
MATa, MAD3-HA3::K.l.URA3, mps1-1	Lab stock	ySP2263
MATa, MAD3-HA3::K.l.URA3, cdc26::K.l.URA3	Lab stock	ySP2268
MATa, myc18-CDC20::TRP1, MAD3-HA3::K.l.URA3	Lab stock	ySP2294
MATa, BUB3-myc18::HIS3, MAD3-HA3::K.l.URA3	Lab stock	ySP2297
MATa, MAD3-HA3::K.l.URA3, cdc5-2::URA3	Lab stock	ySP2514
MATa, MAD3-HA3::K.l.URA3, mps1-1, cdc5-2::URA3	Lab stock	ySP3497
MATa, ura3::4xURA3::GAL1-MAD2	Lab stock	ySP6170
MATa, ura3::4xURA3::GAL1-MAD2, mad1::LEU2	Lab stock	ySP7673
MATa, bar1::hisGURA3hisG, PDS1-myc18::LEU2	Lab stock	ySP7962
MATa, glc7::LEU2, trp1::glc7-10::TRP1	Lab stock	ySP9304
MATα, glc7::LEU2, trp1::glc7-10::TRP1	Lab stock	ySP9305
MATa, MAD3-6Gly-3Flag::KanMX	Lab stock	ySP9960
MATa, ura3::4xURA3::GAL1-MAD2, glc7::LEU2, trp1::glc7-10::TRP1	Lab stock	ySP13415
MATa, bar1::hisGURA3hisG, PDS1-myc18::LEU2, glc7::LEU2, trp1::glc7-10::TRP1	Lab stock	ySP13457
MATa, ura3::4xURA3::GAL1-MAD2, mad3::K.l.TRP1	Lab stock	ySP13458
MATa, glc7::LEU2, trp1::glc7-10::TRP1, MAD3-HA3::K.l.URA3	Lab stock	ySP13548
MATa, glc7::LEU2, trp1::glc7-10::TRP1, MAD3-HA3::K.l.URA3, myc18-CDC20::TRP1	Lab stock	ySP13792
MATa, mad3:: K.l.TRP1, leu2::LEU2::MAD3-S268A	Lab stock	ySP14070
MATa, mad3:: K.l.TRP1, leu2::LEU2::MAD3-S303,S337A	Lab stock	ySP14072
MATa, mad3:: K.l.TRP1, leu2::LEU2::MAD3-S268,S303,S337A	Lab stock	ySP14074
MATa, ura3::4xURA3::GAL1-MAD2, mad3::K.l.TRP1, leu2::LEU2::MAD3-S303,S337A	Lab stock	ySP14168
MATa, ura3::4xURA3::GAL1-MAD2, mad3::K.l.TRP1, leu2::LEU2::MAD3-S268,S303,S337A	Lab stock	ySP14170
MATa, BUB3-HA3::K.l.URA3	Lab stock	ySP14172
MATa, ura3::4xURA3::GAL1-MAD2, mad3::K.l.TRP1, glc7::LEU2, trp1::glc7-10::TRP1	Lab stock	ySP14202
MATa, ura3::4xURA3::GAL1-MAD2, mad1::KanMX, glc7::LEU2, trp1::glc7-10::TRP1	Lab stock	ySP14211
MATa, BUB3-HA3::K.l.URA3, glc7::LEU2, trp1::glc7-10::TRP1	Lab stock	ySP14222
MATa, ura3::4xURA3::GAL1-MAD2, mad3::K.l.TRP1, leu2::LEU2::MAD3-S268A, glc7::LEU2, trp1::glc7-10::TRP1	Lab stock	ySP14328

MATa, ura3::4xURA3::GAL1-MAD2, mad3::K.l.TRP1, leu2::LEU2::MAD3-S268,S303,S33A, glc7::LEU2, trp1::glc7-10::TRP1	Lab stock	ySP14468
MATa, ura3::4xURA3::GAL1-MAD2, mad3::K.l.TRP1, leu2::LEU2::MAD3-S268A	Lab stock	ySP14470
MATa, ura3::4xURA3::GAL1-MAD2, mad3::K.l.TRP1, glc7::LEU2, trp1::glc7-10::TRP1, leu2::LEU2::MAD3-S303,S337A	Lab stock	ySP14545
MATa, MAD3-HA3::K.l.URA3, mps1-1, cdc26::K.l.URA3	Lab stock	ySP14557
MATa, MAD3-6Gly-3Flag::kanMX4, glc7::LEU2, trp1::glc7-10::TRP1	Lab stock	ySP14628
MATα, ura3::4xURA3::GAL1-MAD2, bub3::LEU2	Lab stock	ySP14655
MATα, ura3::4xURA3::GAL1-MAD2, bub1::S.p.HIS5, glc7::LEU2, trp1::glc7-10::TRP1	Lab stock	ySP14663
MATa, ura3::4xURA3::GAL1-MAD2, bub1::S.p.HIS5	Lab stock	ySP14686
MATa, bar1::kanMX, glc7::LEU2, trp1::glc7-10::TRP1	Lab stock	ySP14763
MAT*a, bar1::kanMX4, mad3::K.l.TRP1, leu2::LEU2::MAD3-S268A*	Lab stock	ySP14774
MATa, bar1::kanMX4, mad3::K.l.TRP1, leu2::LEU2::MAD3-S268A, glc7::LEU2, trp1::glc7-10::TRP1	Lab stock	ySP14775
MATa, bar1::kanMX4, mad3::K.l.TRP1, leu2::LEU2::MAD3-S303,S337A	Lab stock	ySP14777
MATa, bar1::kanMX4, mad3::K.l.TRP1, leu2::LEU2::MAD3-S303,S337A, glc7::LEU2, trp1::glc7-10::TRP1	Lab stock	ySP14778
MATa, mad3:: K.l.TRP1, leu2::LEU2::MAD3-S268E	Lab stock	ySP14794
MATa, bar1::kanMX4, mad3::K.l.TRP1, leu2::LEU2::MAD3-S268E	Lab stock	ySP14810
MATa, bar1::kanMX4, mad3::K.l.TRP1	Lab stock	ySP14837
MATa, bar1::kanMX4, myc18-CDC20::TRP1, MAD3-HA3::K.l.URA3	Lab stock	ySP14905
MATα, mad3::K.l.TRP1, leu2::LEU2::MAD3-S268A-HA3::K.l.URA3, myc18-CDC20::TRP1	Lab stock	ySP14966
MATα, mad3::K.l.TRP1, leu2::LEU2::MAD3-S268A-HA3::K.l.URA3, myc18-CDC20::TRP1	Lab stock	ySP14967
MATa, bar1::kanMX4, myc18-CDC20::TRP1, MAD3-HA3::K.l.URA3, glc7::LEU2, trp1::glc7-10::TRP1	Lab stock	ySP15043
MATa, mad3::K.l.TRP1, leu2::LEU2::MAD3-S268A-HA3::K.l.URA3, glc7::LEU2, trp1::glc7-10::TRP1	Lab stock	ySP15072
MATa, mad3::K.l.TRP1, leu2::LEU2::MAD3-S268A-HA3::K.l.URA3	Lab stock	ySP15081
MATα, ura3::4xURA3::GAL1-MAD2, bub3::LEU2, glc7::LEU2, trp1::glc7-10::TRP1	Lab stock	ySP15082
MATα, mad3::K.l.TRP1, leu2::LEU2::MAD3-S268A-HA3::K.l.URA3, BUB3-myc18::HIS3	Lab stock	ySP15161
MATa, mad3::K.l.TRP1, leu2::LEU2::MAD3-S268E-HA3::K.l.URA3	Lab stock	ySP15331
MATα, mad3::K.l.TRP1, leu2::LEU2::MAD3-S268E-HA3::K.l.URA3, myc18-CDC20::TRP1	Lab stock	ySP15373

MATa, bar1::kanMX4, mad3::K.l.TRP1, leu2::LEU2::MAD3-S268E, glc7::LEU2, trp1::glc7-10::TRP1	Lab stock	ySP15388
MATa, myc18-CDC20::TRP1, MAD3-HA3::K.l.URA3, cdc5-2::URA3	Lab stock	ySP15444
MATa, myc18-CDC20::TRP1, MAD3-HA3::K.l.URA3, mps1-1	Lab stock	ySP15446
MATa, myc18-CDC20::TRP1, MAD3-HA3::K.l.URA3, cdc5-2::URA3, mps1-1	Lab stock	ySP15449
MATa, BUB3-HA3::K.l.URA3, myc18-CDC20::TRP1, bar1::kanMX4	Lab stock	ySP15499
MATa, BUB3-HA3::K.l.URA3, myc18-CDC20::TRP1, bar1::kanMX4, glc7::LEU2, trp1::glc7-10::TRP1	Lab stock	ySP15512
Oligonucleotides		
Primers for PCR, see Table S1		
Recombinant DNA		
NDC10-HA3 cloned in pRS304	This paper	pSP62
MAD3 cloned in Yiplac128	This paper	pSP1395
MAD3-S268A cloned in Yiplac128	This paper	pSP1396
MAD3-S268E cloned in Yiplac128	This paper	pSP1397
MAD3-S330,S337A cloned in Yiplac128	This paper	pSP1398
MAD3-S268,S330,S337A cloned in Yiplac128	This paper	pSP1400
Software and Algorithms		
ImageJ		https://imagej.nih.gov/ij/
MaxQuant		https://www.maxquant.org/
Skyline software v4.1.0.11717		https://skyline.ms/project/home/software/Skyline/begin.view

Figure 1

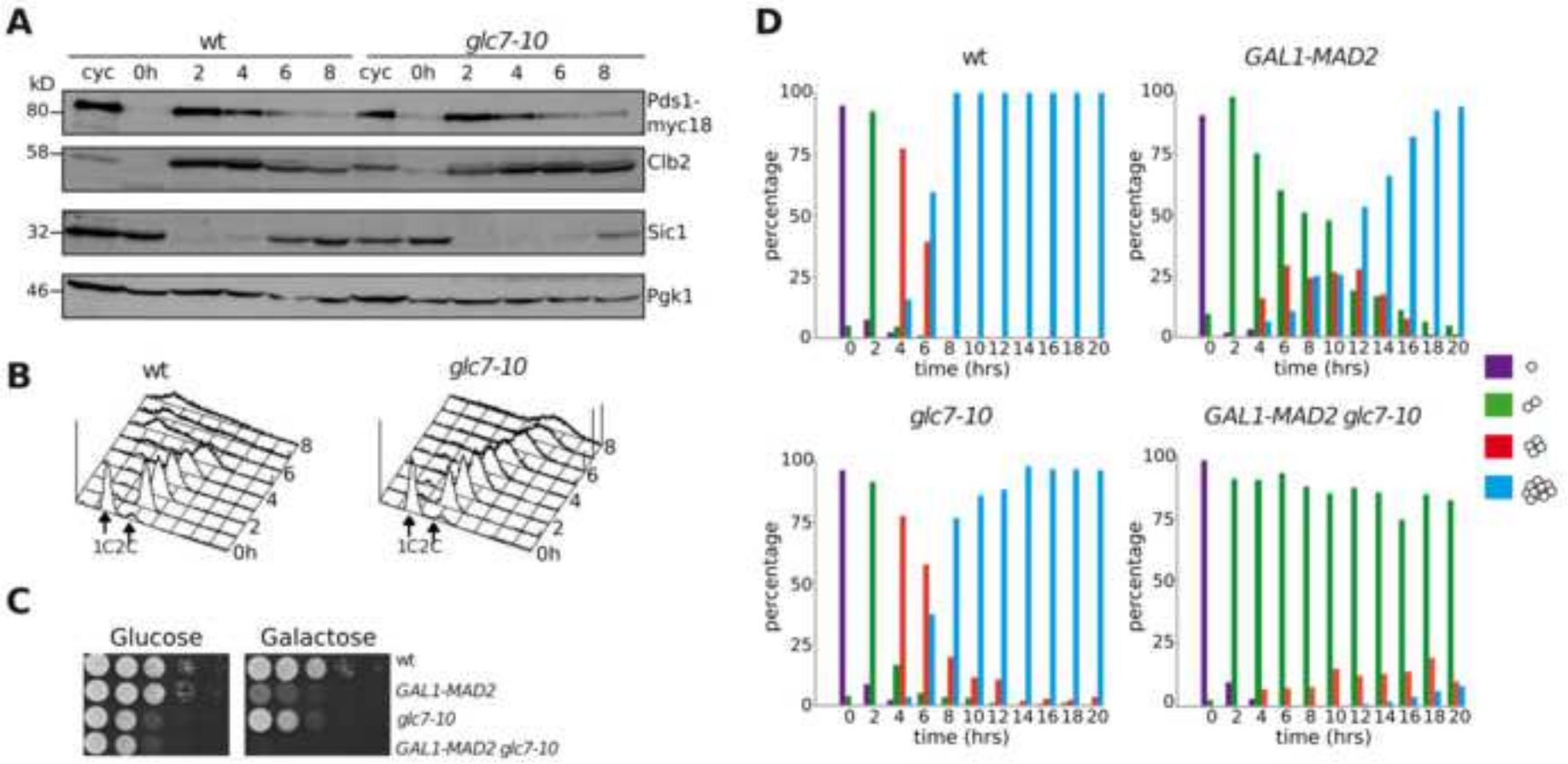

Figure 2

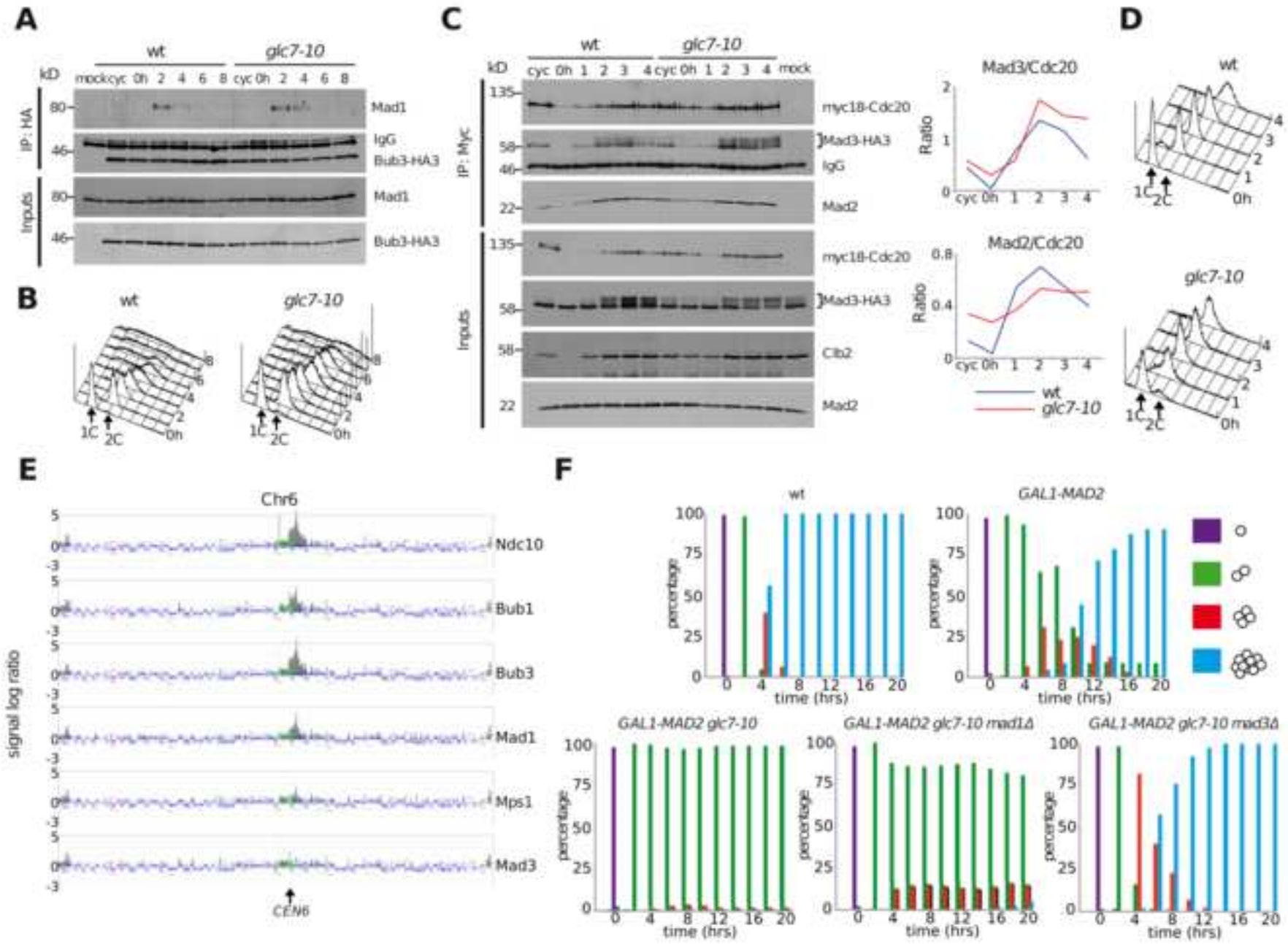

Figure 3

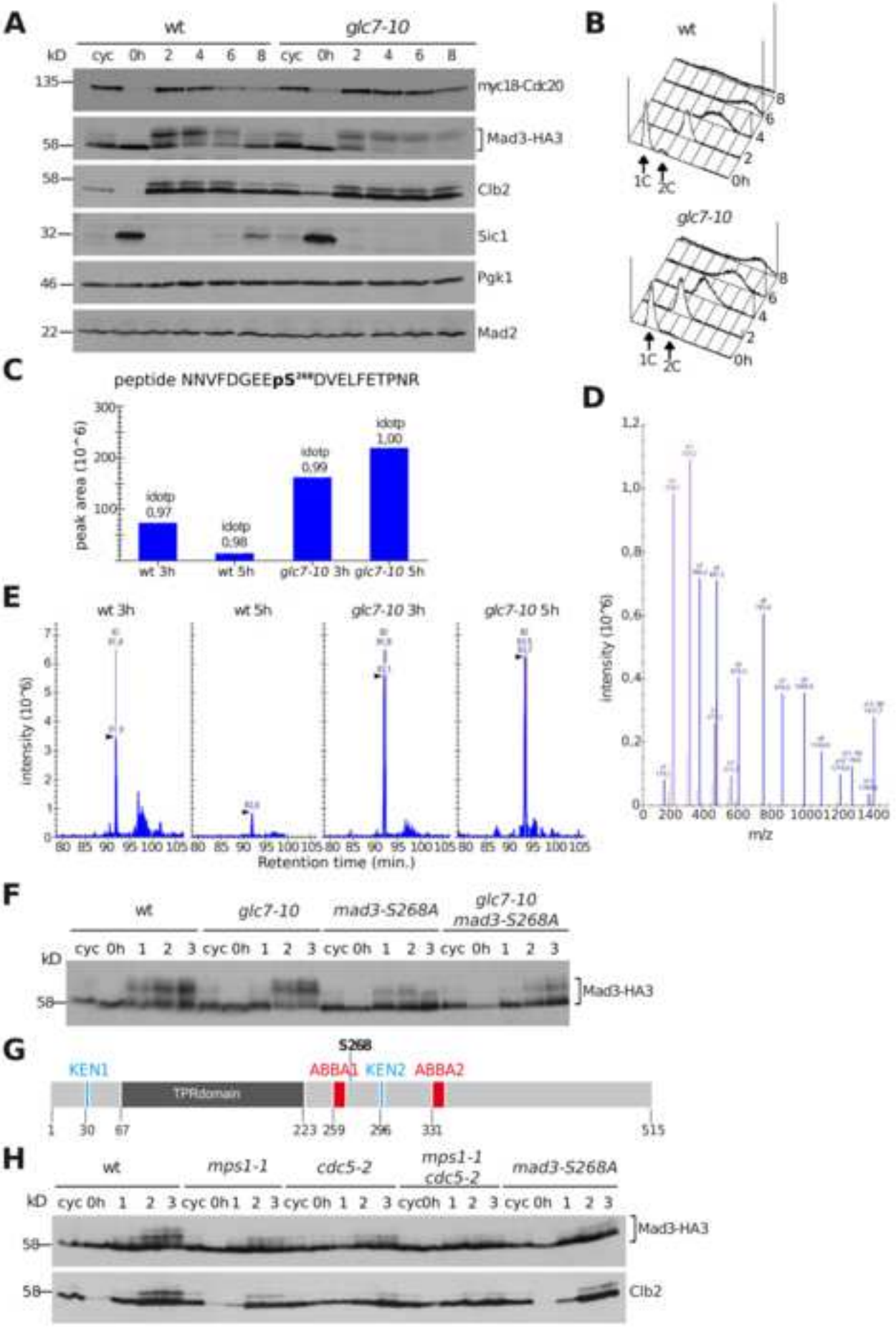

Figure 4

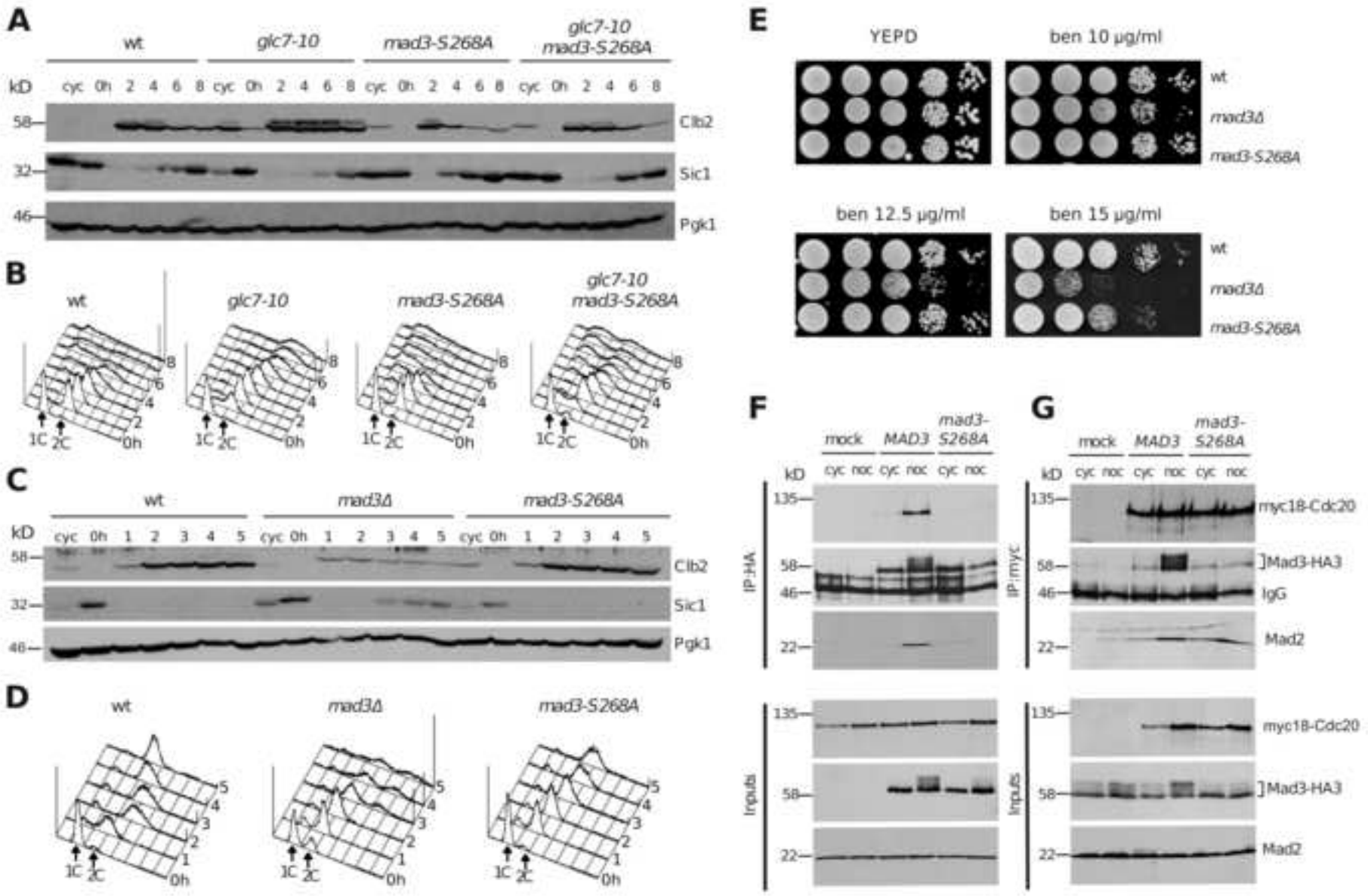

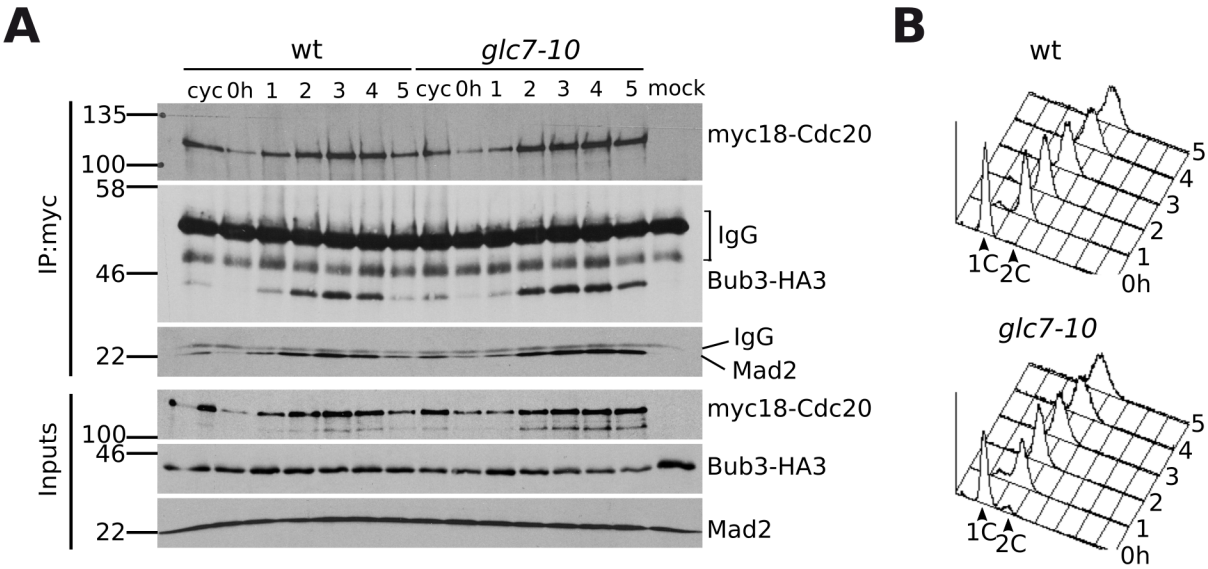
A
wt
glc7-10
cyc 0h 1 2 3 4 5 cyc 0h 1 2 3 4 5 mock
135
100
58
46
22
IP:myc
myc18-Cdc20
IgG
Bub3-HA3
IgG
Mad2
Inputs
100
46
22
myc18-Cdc20
Bub3-HA3
Mad2
B
wt
5
4
3
2
1
0h
1C
2C
glc7-10
5
4
3
2
1
0h
1C
2C

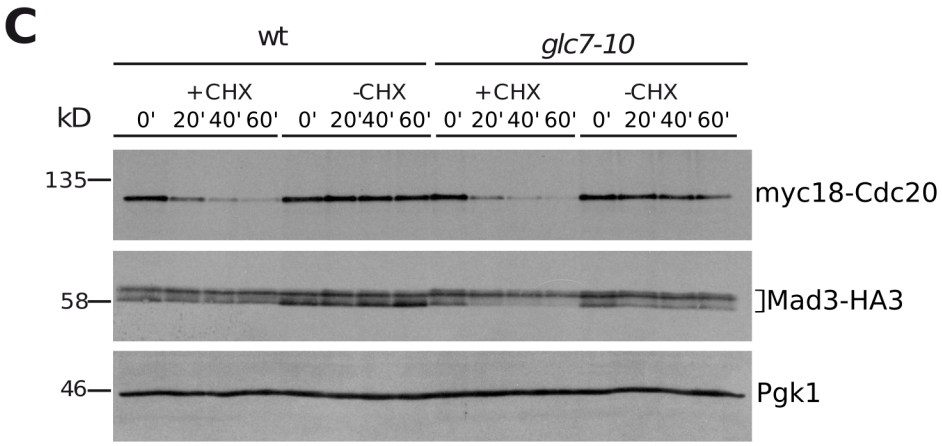
C
wt
glc7-10
+CHX -CHX +CHX -CHX
kD
0' 20' 40' 60' 0' 20' 40' 60' 0' 20' 40' 60' 0' 20' 40' 60'
135
58
46
myc18-Cdc20
]Mad3-HA3
Pgk1

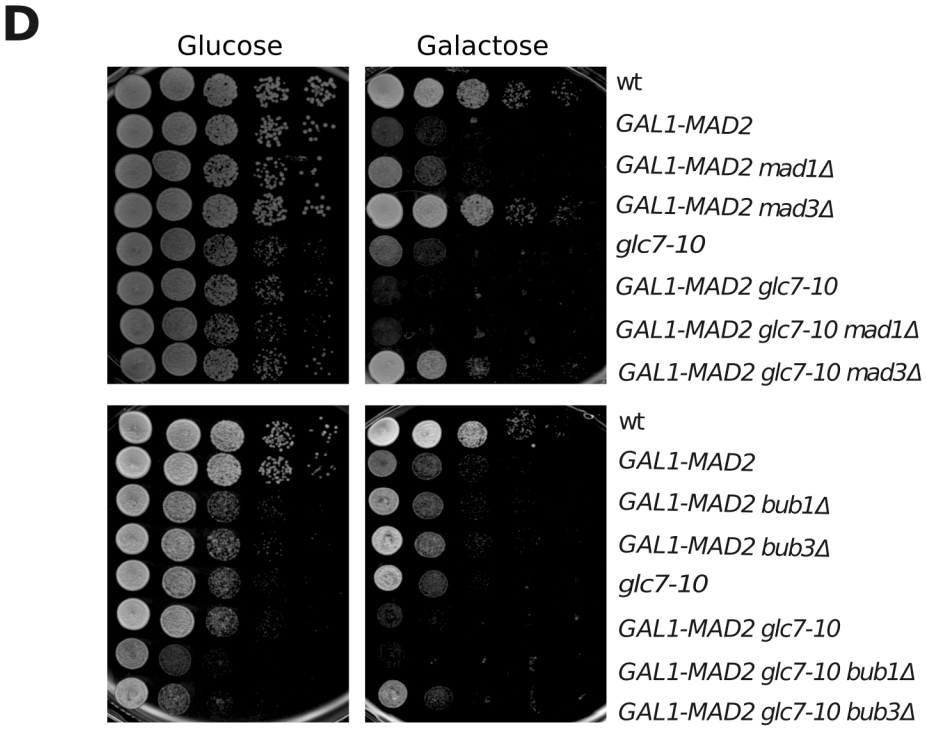
D
Glucose
Galactose
wt
GAL1-MAD2
GAL1-MAD2 mad1Δ
GAL1-MAD2 mad3Δ
glc7-10
GAL1-MAD2 glc7-10
GAL1-MAD2 glc7-10 mad1Δ
GAL1-MAD2 glc7-10 mad3Δ
wt
GAL1-MAD2
GAL1-MAD2 bub1Δ
GAL1-MAD2 bub3Δ
glc7-10
GAL1-MAD2 glc7-10
GAL1-MAD2 glc7-10 bub1Δ
GAL1-MAD2 glc7-10 bub3Δ

Figure S1. *glc7-10* cells show normal Cdc20 turnover and their slippage defects is kinetochore-independent. Related to Figure 2.

(A-B): Wild-type (ySP15499) and *glc7-10* mutant (ySP15512) expressing myc-tagged Cdc20 (myc18-Cdc20) and HA-tagged Bub3 (Bub3-HA3) were grown at 25°C, arrested in G1 with α-factor and released at 30°C in the presence of benomyl (t=0). Two hours after release α-factor (2μg/ml) was re-added to block cells that were slipping out of mitosis in the next G1 phase. Samples were collected at the indicated times to analyse the interaction of Bub3-HA3 with myc18-Cdc20 by co-immunoprecipitations (A). Throughout the time course, DNA contents were measured by FACS analysis (B). Cdc20 was immunoprecipitated with an anti-myc antibody and immunoprecipitates (IP) and inputs were probed by western blot with anti-myc, anti-HA and anti-Mad2 antibodies (A). As negative control (mock), nocodazole-arrested cells expressing untagged Cdc20 and Bub3-HA3 (ySP1346) were used. Inputs represent 1/50th of the extracts used for IPs. **(C):** Wild-type (ySP2294) and *glc7-10* mutant cells (ySP13792) expressing myc18-Cdc20 and Mad3-HA3 were arrested in mitosis by nocodazole treatment at 30°C. At time 0 cycloheximide (CHX) was added to half of the cultures and samples were collected at indicated times for western blot analysis with anti-myc and anti-HA antibodies. Pgk1 was used as loading control. **(D):** Serial dilutions of cells with the indicated genotypes were spotted on YEPD (glucose) or YEPG (galactose) and incubated at 30°C.

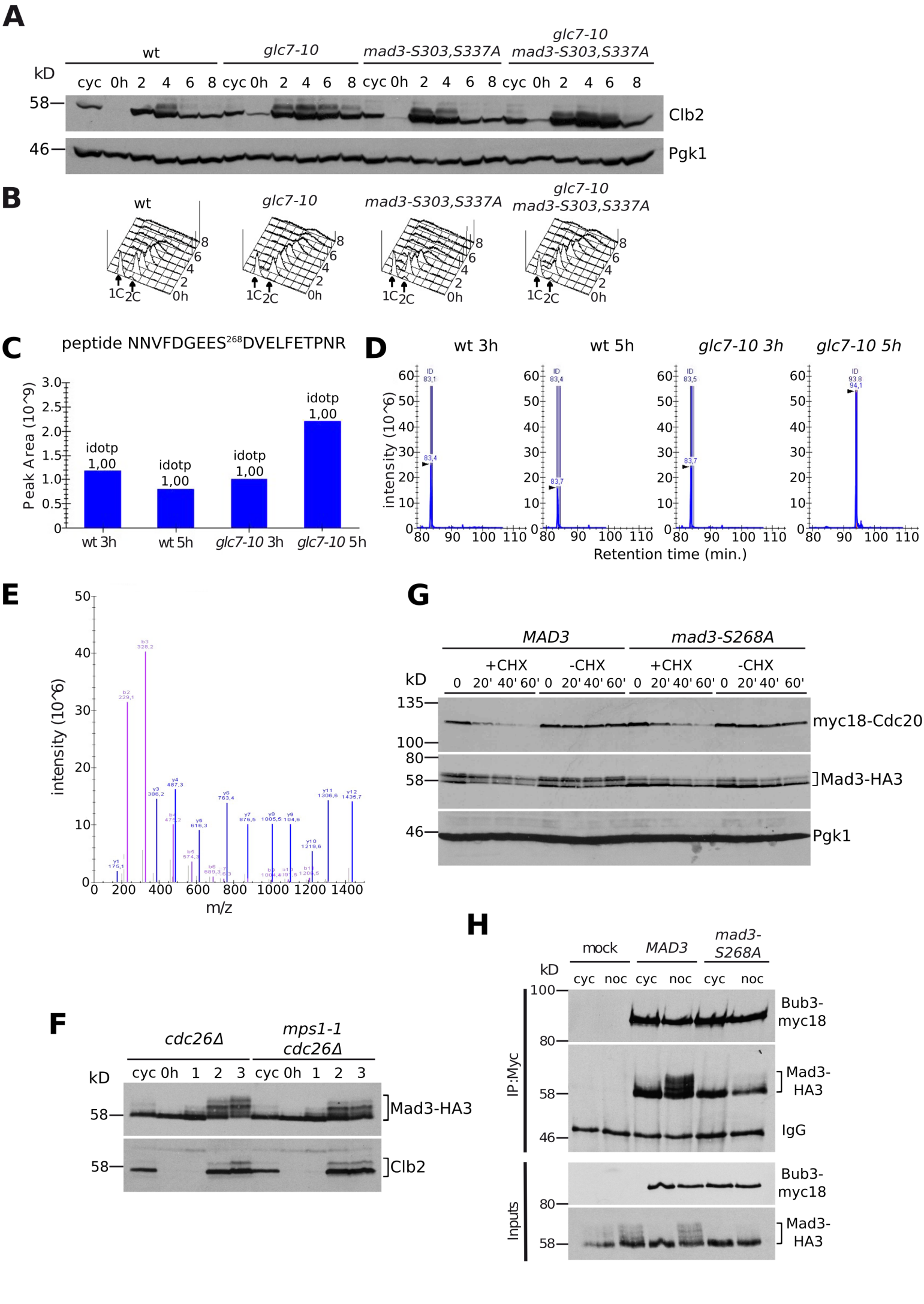
A
wt
glc7-10
mad3-S303,S337A
glc7-10 mad3-S303,S337A
kD
cyc 0h 2 4 6 8 cyc 0h 2 4 6 8 cyc 0h 2 4 6 8 cyc 0h 2 4 6 8
58
Clb2
46
Pgk1
B
wt
glc7-10
mad3-S303,S337A
glc7-10 mad3-S303,S337A
1C 2C 0h 2 4 6 8
C
peptide NNVFDGEES[268]DVELFETPNR
Peak Area (10^9)
idotp 1,00
wt 3h
wt 5h
glc7-10 3h
glc7-10 5h
D
wt 3h
wt 5h
glc7-10 3h
glc7-10 5h
intensity (10^6)
Retention time (min.)
E
intensity (10^6)
m/z
G
MAD3
mad3-S268A
+CHX
-CHX
kD
0 20' 40' 60' 0 20' 40' 60' 0 20' 40' 60' 0 20' 40' 60'
135
100
80
58
46
myc18-Cdc20
]Mad3-HA3
Pgk1
H
mock
MAD3
mad3-S268A
kD
cyc noc cyc noc cyc noc
100
80
58
46
IP:Myc
Bub3-myc18
Mad3-HA3
IgG
Inputs
Bub3-myc18
Mad3-HA3
F
cdc26Δ
mps1-1 cdc26Δ
kD
cyc 0h 1 2 3 cyc 0h 1 2 3
58
Mad3-HA3
58
]Clb2

Figure S2. Impact of Mad3 phosphorylation on Mad3 stability and mitotic slippage. Related to Figures 3 and 4.

(A-B): Wild-type (ySP1056), *glc7-10* (ySP14763), *mad3-S303,S337A (*ySP14777) and *glc7-10 mad3-S303,S337A (*ySP14778*)* cells were grown at 25°C, arrested in G1 with α-factor and released at 30°C in the presence of benomyl (t=0). α-factor (2 μg/ml) was re-added after 2h to arrest cells in the next G1 after slippage. Samples were collected at the indicated times for Western blot analysis of Clb2 and Pgk1 (loading control) (A), as well as for FACS analysis of DNA contents (B). **(C-E):** MS/MS analysis of the Mad3 peptide NNVFVDGEESDVELFETPNR (extracted by precursor ion M at m/z 1155,5297 ++). The Isotope Dot Product (idotp, C) allows to assess the distribution of the precursor isotope and its correlation between expected and observed pattern, with optimal matching resulting in an idotp value =1. Chromatograms and peak intensity traces for the four samples (wt 3hrs, wt 5 hrs, *glc7-10* 3hrs and *glc7-10* 5hrs) are displayed (D). The extracted ion chromatograms for isotope peaks at m/z 1155,5297 are displayed for each condition after MS1 filtering for peptide NNVFVDGEESDVELFETPNR. The vertical lines with annotated retention times and identification (ID) mark underlying MS/MS sampling that initially directed MS1 peak picking. The skyline (E) displays a library of MS/MS spectra for the selected peptide that provides underlying peptide identification information for a specific condition (in this case *glc7-10* at 5hrs of benomyl treatment). **(F):** *cdc26Δ* (ySP2268) and *mps1-1 cdc26Δ* cells (ySP14557) were grown at 25°C, arrested in G1 with α-factor and released at 37°C in the presence of nocodazole (t=0). Samples were collected at the indicated times for western blot analysis of Mad3 with anti-HA and anti-Clb2 antibodies. Clb2 was used as a mitotic marker. **(G):** Wild-type (ySP2294) and *mad3-S268A* mutant cells (ySP14966) expressing myc18-Cdc20 and Mad3-HA3 were arrested in mitosis by nocodazole treatment at 30°C. At time 0 cycloheximide (CHX) was added to half of the cultures and samples were collected at indicated times for

western blot analysis with anti-myc and anti-HA antibodies. Pgk1 was used as loading control. **(H):** Cycling cultures (cyc) of wild type (ySP2297) and *mad3-S268A* mutant cells (ySP15161) expressing myc-tagged Bub3 (Bub3-myc18) and HA-tagged Mad3 (Mad3-HA3), were treated with nocodazole (noc) at 25°C for 3h. As negative controls (mock), cycling and nocodazole-arrested cells expressing Mad3HA3 (ySP2220) were used. Bub3 was immunoprecipitated from the extracts with an anti-myc antibody. Immunoprecipitates (IP) along with the Inputs ($1/50^{th}$ of the extracts used for IPs), were immunoblotted with anti-HA and anti-myc antibodies.

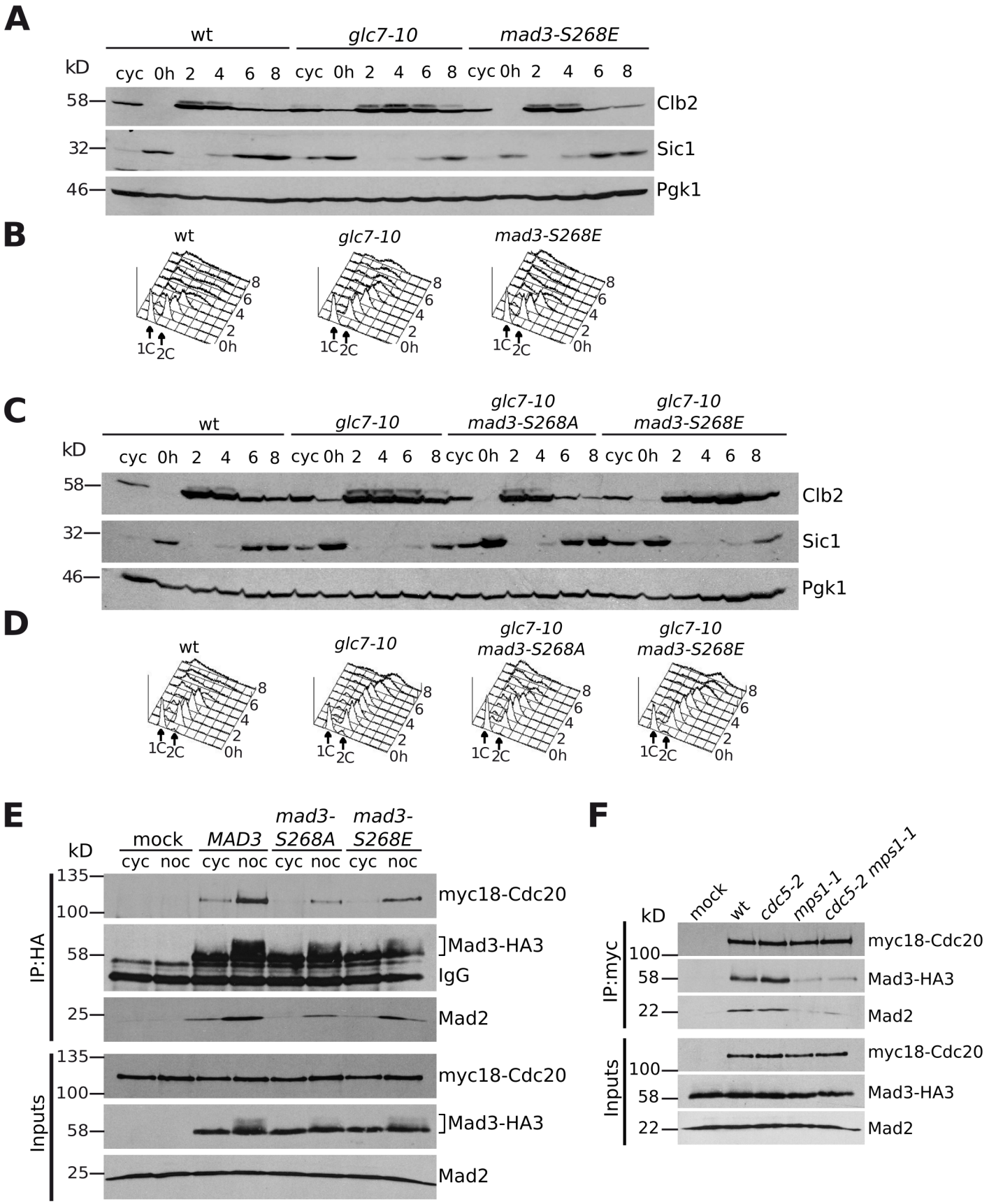
A
wt
glc7-10
mad3-S268E
kD
cyc 0h 2 4 6 8 cyc 0h 2 4 6 8 cyc 0h 2 4 6 8
58
32
46
Clb2
Sic1
Pgk1
B
wt
glc7-10
mad3-S268E
8
6
4
2
0h
1C
2C
C
wt
glc7-10
glc7-10 mad3-S268A
glc7-10 mad3-S268E
kD
cyc 0h 2 4 6 8 cyc 0h 2 4 6 8 cyc 0h 2 4 6 8 cyc 0h 2 4 6 8
58
32
46
Clb2
Sic1
Pgk1
D
wt
glc7-10
glc7-10 mad3-S268A
glc7-10 mad3-S268E
8
6
4
2
0h
1C
2C
E
kD
mock
MAD3
mad3-S268A
mad3-S268E
cyc noc cyc noc cyc noc cyc noc
IP:HA
135
100
58
25
myc18-Cdc20
]Mad3-HA3
IgG
Mad2
Inputs
135
100
58
25
myc18-Cdc20
]Mad3-HA3
Mad2
F
kD
mock
wt
cdc5-2
mps1-1
cdc5-2 mps1-1
IP:myc
100
58
22
myc18-Cdc20
Mad3-HA3
Mad2
Inputs
100
58
22
myc18-Cdc20
Mad3-HA3
Mad2

Figure S3. The *mad3-S268E* mutant does not behave as phosphomimetic. Related to Figure 4.

(A-B): Wild-type (ySP1056), *glc7-10* (ySP14763), and *mad3-S268E* (ySP14810) cells were grown at 25°C, arrested in G1 with α-factor and released at 30°C in the presence of benomyl (t=0). α-factor (2 μg/ml) was re-added after 2h to arrest cells in the next G1 after slippage. Samples were collected at the indicated times for western blot analysis of Clb2 and Pgk1 (loading control) (A), as well as for FACS analysis of DNA contents (B). **(C-D):** Wild-type (ySP1056), *glc7-10* (ySP14763), *glc7-10 mad3-S268A* (ySP14775) and *glc7-10 mad3-S268E* (ySP15388*)* cells were treated as in (A). Samples were collected at the indicated times for Western blot analysis of Clb2, Sic1 and Pgk1 (loading control) (C), as well as for FACS analysis of DNA contents (D). **(E):** Cycling cultures (cyc) of wild type (ySP2294) , *mad3-S268A* (ySP14967) and *mad3-S268E* (ySP15373) mutant cells expressing myc-tagged Cdc20 (myc18-Cdc20) and HA-tagged Mad3 (Mad3-HA3), were treated with nocodazole (noc) at 25°C for 3h. As negative control (mock), cycling and nocodazole-arrested cells expressing myc18-Cdc20 (ySP1414) were used. Mad3 was immunoprecipitated from the extracts with an anti-HA antibody. Immunoprecipitates (IP) along with the Inputs ($1/50^{th}$ of the extracts used for IPs), were immunoblotted with anti-HA, and anti-myc and anti-Mad2 antibodies. **(F):** Cycling cultures (cyc) of wild type (ySP2294) , *cdc5-2* (ySP15444), *mps1-1* (ySP15446) and *cdc5-2 mps1-1* (ySP15449) mutant cells expressing myc-tagged Cdc20 (myc18-Cdc20) and HA-tagged Mad3 (Mad3-HA3) were arrested in G1 with α-factor and released at 37°C in the presence of nocodazole for 90 minutes (time at which all strains are in mitosis). As negative control (mock), cycling and nocodazole-arrested cells expressing Mad3-HA3 (ySP2220) were used. Cdc20 was immunoprecipitated from the extracts with an anti-myc antibody. Immunoprecipitates (IP) along with the Inputs ($1/50^{th}$ of the extracts used for IPs), were immunoblotted with anti-HA, and anti-myc and anti-Mad2 antibodies.

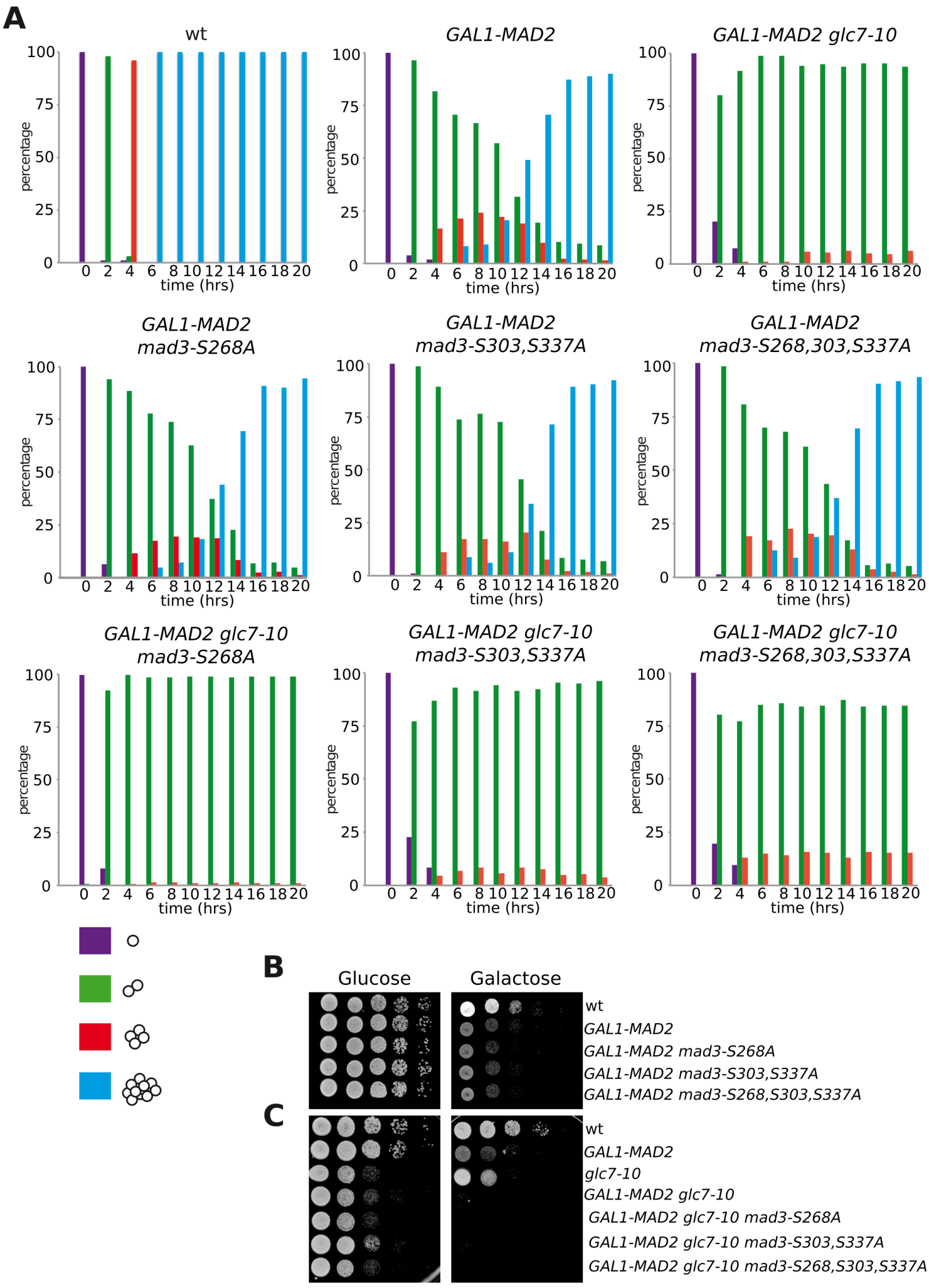
A
wt
GAL1-MAD2
GAL1-MAD2 glc7-10
GAL1-MAD2 mad3-S268A
GAL1-MAD2 mad3-S303,S337A
GAL1-MAD2 mad3-S268,303,S337A
GAL1-MAD2 glc7-10 mad3-S268A
GAL1-MAD2 glc7-10 mad3-S303,S337A
GAL1-MAD2 glc7-10 mad3-S268,303,S337A
percentage
time (hrs)
0 2 4 6 8 10 12 14 16 18 20
0 25 50 75 100
B
Glucose
Galactose
wt
GAL1-MAD2
GAL1-MAD2 mad3-S268A
GAL1-MAD2 mad3-S303,S337A
GAL1-MAD2 mad3-S268,S303,S337A
C
wt
GAL1-MAD2
glc7-10
GAL1-MAD2 glc7-10
GAL1-MAD2 glc7-10 mad3-S268A
GAL1-MAD2 glc7-10 mad3-S303,S337A
GAL1-MAD2 glc7-10 mad3-S268,S303,S337A

Figure S4. *MAD2* overexpression restores normal slippage in *mad3-S268A* cells. Related to Figure 4.

(A): Strains with the indicated genotypes were grown in uninduced conditions (YEPR) at 25°C, arrested in G1 with α-factor and spotted on YEPG plates that were incubated at 30°C from the time of release (t=0) to allow microcolonies formation. 200 cells were scored at each time point to determine the percentage of single cells (purple) and of microcolonies of two (green), four (red), or more than four cells (blue). **(B-C):** Serial dilutions of cells with the indicated genotypes (same strains as in (A)) were spotted on YEPD (glucose) or YEPG (galactose) and incubated at 30°C.

Table S1. Primers used in this study for gene tagging. Related to STAR Methods.

SP63 (for tagging *BUB3* with *3HA::K.l.URA3*; fwd):

ACGCCGCAATTGACCAAACTATTGAACTAAACGCAAGTTCAATATACATAATATTTGACTATGA

GAAC**TCCGGTTCTGCTGCTAG**

SP64 (for tagging *BUB3* with *3HA::K.l.URA3*; rev):

GAGAGAGCGATGAATCTGAATTTTTTTTCTGGAATGTTCTATCATACTACACGAATCTTCACGA

AGATA**CCTCGAGGCCAGAAGAC**

SP84(for tagging *BUB1* with *3HA::K.l.URA3*; fwd):

ACGTAATTCTAAGCATTGAAGAGGAGTTATCACATTTTCAATATAAGGGGAAACCGTCAAGGAG

ATTT**TCCGGTTCTGCTGCTAG**

SP85(for tagging *BUB1* with *3HA::K.l.URA3*; rev):

GTCATTGCTATGGAATCTGGCAGGACACCAAAAAGTCACCTATGCGGGAGATGAAGGCATATTT

ATTCA**CCTCGAGGCCAGAAGAC**

SP134 (for tagging *MAD1* with *3HA::K.l.URA3*; fwd):

GATAGAGGTCAACTTCCGTGCTTTTTGGCAACAATAACATTGCGTCTGTGGGAACAGCGACAAG

CCAAA**TCCGGTTCTGCTGCTAG**

SP135 (for tagging *MAD1* with *3HA::K.l.URA3*; rev):

ATGTCAGCGGATAGGAGTTTATCATATTATAAAACCGATTACTATTATCTATTAGAAATGTATA

TACAC**CCTCGAGGCCAGAAGAC**

SP138 (for tagging *MAD3* with *3HA::K.l.URA3*; fwd):

AAAAATTCTGAGATCATTTCAGATGATGACAAGTCGAGTTCGTCTTTCATATCGTACCCACCACA

GCGT**TCCGGTTCTGCTGCTAG**

SP139 (for tagging *MAD3* with *3HA::K.l.URA3*; rev):

AAAAAAGTCGGCCGTCGATGTGTTTACGATTGGCCAGTATACTTACTCATTCATGGGATTAGTT

TTATT**CCTCGAGGCCAGAAGAC**

SP299 (for cloning *MAD3* CDS with 5' UTR and 3' UTR; rev):

CGGAATTCGTATGTCATAAGCGTTAATCGGAC

SP329 (for cloning *MAD3* CDS with 5' UTR and 3' UTR; fwd):

GGAATTCGAAAGAACCTACCTGTCTTGG

MP243 (for tagging *MAD3* with 6Gly-3Flag; fwd):

TCAGATGATGACAAGTCGAGTTCGTCTTTCATATCGTACCCACCACAGCGT**GGGGGAGGCGGGGGTGGA**

MP244 (for tagging *MAD3* with 6Gly-3Flag; rev):

TGTGTTTACGATTGGCCAGTATACTTACTCATTCATGGGATTAGTTTTTTA**GAATTCGAGCTCGTTTAAAC**

Sequences in bold anneal to the cassette-bearing plasmid

Supplemental Video 1

Click here to access/download

Supplemental Videos and Spreadsheets

Movie S1.avi